DEVELOPMENTAL BIOLOGY

The BMP ligand Pinhead together with Admp supports the robustness of embryonic patterning

Yifang Yan[1], Guozhu Ning[1], Linwei Li[1], Jie Liu[1], Shuyan Yang[1], Yu Cao[1], Qiang Wang[1,2]*

Vertebrate embryonic dorsoventral axis is robustly stable in the face of variations in bone morphogenetic protein (BMP) signaling. However, the molecular mechanism behind this robustness remains uncharacterized. In this study, we show that zebrafish Pinhead, together with Admp, plays an important compensatory role in ensuring the robustness of axial patterning through fine-tuning of BMP signaling. *pinhead* encodes a BMP-like ligand expressed in the ventrolateral margin of the early gastrula. Transcription of *pinhead* and *admp* is under opposing regulation, where *pinhead* depletion results in a compensatory increase in *admp* transcription and vice versa, leading to normal axis formation in *pinhead* or *admp* mutants. Expression of *pinhead* and *admp* is directly repressed by the BMP/Smad pathway. When BMP signals were inhibited or excessively activated, *pinhead/admp* expression changed accordingly, allowing for self-regulation. Thus, this study reveals a negative feedback loop between BMP signaling and *pinhead/admp* that effectively stabilizes embryonic patterning by buffering against fluctuations in BMP signaling.

INTRODUCTION

Bone morphogenetic proteins (BMPs), originally identified by their ability to induce ectopic bone formation, are multifunctional extracellular polypeptides that belong to the transforming growth factor–β (TGF-β) superfamily (*1*). Secreted BMP ligands bind as dimers to type I and type II receptors on the cell surface. The type II receptors become phosphorylated and then activate the type I receptors, which in turn phosphorylate the regulatory Smads (Smad1/5/8) (*2*). These phosphorylated Smads form complexes with Smad4, which then translocate into the nucleus to regulate the expression of BMP target genes (*2*). In zebrafish, *bmp2b* and *bmp7a*, which function as BMP heterodimers that activate Smad1/5, are initially expressed throughout the blastoderm shortly after the midblastula transition (*3*). BMP signaling in dorsal regions is subsequently attenuated by the BMP antagonist Chordin (Chd), and then a BMP signaling gradient forms along the dorsoventral (DV) axis and patterns tissues with high levels ventrally and low levels dorsally during late blastula stages and before the onset of gastrulation (*3*, *4*). Although many positive and negative regulators of BMP signaling have been identified during early embryonic development (*4*), the molecular network that generates and maintains the BMP gradient is still not well characterized.

The formation of a morphogen gradient is a dynamic process and is influenced by the kinetics of morphogen production, diffusion, and degradation. During embryonic development, the formation of a morphogen gradient is often challenged by signaling component-level fluctuations, temperature differences, size variations, and/or unequal distributions of components between daughter cells (*5*). Therefore, morphogen gradients should be reproducibly formed with robust stability from one embryo to the next (*5*). Specifically, a robust resistance of DV axis formation to perturbations has been observed in various vertebrate embryos during classic grafting and ablation experiments. When grafted to the ventral-most part of a host embryo, where the BMP signal is maximally activated, the Spemann-Mangold organizer of *Xenopus* and the embryonic shield of zebrafish retain their ability to induce a secondary body axis at the site of the graft (*6*, *7*). Furthermore, even when an amphibian blastula is bisected into dorsal and ventral halves, the dorsal half can give rise to a well-proportioned half-sized embryo (*8*). In addition, avian embryos can compensate for the removal of the organizer (Hensen's node) during the primitive streak stage as evidenced by the reappearance of organizer markers (*9*). These observations support the idea that self-regulation occurs on the dorsal side of vertebrate embryos. On the other hand, transplantation of zebrafish ventral margin cells into animal poles induces the formation of secondary tails, indicating the existence of a tail organizer (*10*). Therefore, both the ventral and dorsal sides of vertebrate embryos are involved in self-regulation of DV patterning, but the underlying mechanism ensuring the robust BMP activity gradient remains one of the great unsolved mysteries in developmental biology.

In zebrafish embryos, ventral BMP signaling maintains expression of the *vox/vent/ved* transcriptional repressors, which restrict the expression of dorsal-promoting genes, including *chd* (*11*). In *Xenopus*, the expression of *chd* is negatively regulated by BMP4 (*8*). Therefore, the BMP signal gradient controlled by ventral BMP ligands and their dorsally secreted antagonist Chd is theoretically unstable, where a small change in the BMP signals or Chd expression would cause severe defects in the DV body plan (*12*). A BMP-like protein, anti-dorsalizing morphogenetic protein (Admp), is uniquely expressed in and secreted by the dorsal organizer (*13*, *14*). Admp associates with Chd and facilitates Chd degradation (*15*). The expression of *admp* is repressed by BMP signals, and a depletion of the ventral BMP signals will increase *admp* expression, thus allowing the regeneration of a new BMP signal gradient. Therefore, Admp is an appealing candidate for ensuring the stabilization of DV patterning (*8*). Unexpectedly, knockdown of *admp* in *Xenopus* or zebrafish using morpholinos (MOs) only causes mild dorsalization (*8*, *12*, *16*, *17*), and the distribution of the Chd protein remains largely unchanged (*17*), suggesting that there are other BMP-like members that compensate for the loss of Admp function. In addition, the dorsal halves of split *Xenopus* embryos still retain substantial DV polarity when

[1]State Key Laboratory of Membrane Biology, Institute of Zoology, University of Chinese Academy of Sciences, Chinese Academy of Sciences, Beijing 100101, China
[2]Institute for Stem Cell and Regeneration, Chinese Academy of Sciences, Beijing 100101, China
*Corresponding author. Email: qiangwang@ioz.ac.cn

BMP4 and BMP7 are depleted (*8*), indicating that unidentified BMP-like members may function in the newly induced ventral side and are transcriptionally up-regulated to compensate for the loss of BMP ligands.

The precursor proteins of BMP family members consist of three parts: an N-terminal signal peptide that targets the protein to the secretory pathway, a prodomain that mediates proper folding, and a C-terminal mature peptide containing seven highly conserved cysteines, i.e., cysteine knots, that form intramolecular disulfide bonds (*18*). In addition, an Arg-X-X-Arg sequence motif in the prodomain of the precursor proteins is hydrolyzed by serine proteinases to form mature C-terminal proteins that are subsequently secreted (*18*). There are at least 20 structurally and functionally related BMPs, including Decapentaplegic, Screw, and Glassbottom-boat in *Drosophila* and BMP2/4, BMP5/6/7/8, and BMP9/10 in vertebrates. Most of these BMPs play critical roles in embryogenesis and organ morphogenesis (*19*–*21*). The characterization of previously unknown BMP members involved in embryonic development will be interesting and provide key insights into this developmental pathway.

The novel gene *pinhead* was originally isolated from a functional knockdown screen searching for genes involved in nervous system development and is expressed in the anterior neural plate of *Xenopus* neurula as a key regulator of head development (*22*). *pinhead* is located immediately upstream of *admp* in the genomes of various animals, ranging from arthropods to vertebrates (*22*, *23*). This genomic configuration of *pinhead* and *admp* is important for mutually exclusive expression of these genes in *Ciona* embryos, which lack a structure homologous to the vertebrate organizer (*23*). In gastrulating *Xenopus* embryos, *pinhead* is expressed in an arc around the blastopore with a distinct gap corresponding to the dorsal mesoderm, which implies a possible role in the embryonic body plan (*22*).

In this study, we demonstrated that Pinhead is a secreted BMP-like ligand expressed in the ventrolateral margin and has ventralizing functions in the zebrafish embryonic body plan. Similar to Admp, Pinhead was also found to promote metalloproteinase-mediated Chd degradation. Expression of *pinhead* was notably increased in response to the inhibition or depletion of *admp* and vice versa. This "seesaw"-like expression of *pinhead* and *admp* establishes a well-orchestrated alternative mechanism for the robust generation of the DV axis. This is evidenced by the normal DV polarity exhibited by *pinhead* or *admp* mutants alongside the marked dorsalization displayed when both of these genes are absent. Last, the expression of *pinhead* and *admp* is negatively regulated by BMP signaling, where this negative feedback loop between BMP signaling and *pinhead/admp* is important for buffering against fluctuations in dynamic BMP signaling during DV axis formation. Therefore, we propose an alternative mechanism to ensure stable axis formation that couples *pinhead* and *admp* with system control based on opposing regulation of BMP signaling and *pinhead/admp* expression. This work will provide important insights into the mechanisms of robustness in organisms by the self-regulating BMP activity gradient.

RESULTS

Zebrafish *pinhead* is a ventralizing gene expressed in the ventrolateral margin

Expression of *pinhead* and *admp* occurs in a mutually exclusive manner during *Ciona* and *Xenopus* embryonic development (*22*, *23*). Admp is a BMP-like protein with important functions in the embryonic body plan (*13*, *14*, *16*). However, the developmental role of *pinhead* in DV patterning remains unknown. To gain insight into the functions of zebrafish *pinhead* [NM_205587.1, National Center for Biotechnology Information (NCBI)] during embryogenesis, we firstly characterized its expression during early embryonic development using whole-mount in situ hybridization (WISH) with an antisense probe. As shown in Fig. 1A, *pinhead* transcripts were undetectable before and during the sphere stage. Soon afterward, *pinhead* was expressed around the marginal zone but not the dorsal mesoderm, as indicated by costaining with *goosecoid* (*gsc*) (Fig. 1, A and B). During the midgastrulation stages, the expression of *pinhead* transcripts appeared in a DV gradient in the blastoderm margin (Fig. 1A). Abundant *pinhead* transcripts were consistently observed in the presomitic mesoderm, but not the axial mesoderm, at the bud stage and during somitogenesis (Fig. 1A and fig. S1A). *pinhead* transcripts were no longer detectable after the segmentation stages (fig. S1B). These data indicate that zebrafish *pinhead* may play a role in establishing ventral cell fates during early embryonic development.

Next, the effects of *pinhead* overexpression on embryogenesis were assessed by injecting mRNA synthesized in vitro into one-cell stage embryos. Embryos injected with different amounts of *pinhead* mRNA exhibited dose-dependent ventralized phenotypes, characterized by the loss of dorsoanterior structures and the expanded ventral tissues at 24 hours post-fertilization (hpf) (Fig. 1, C and D), suggesting that Pinhead protein has ventralizing activity. In contrast to the impaired function of BMP2b by the addition of six amino acids at its C terminus in *swirl* mutants (*24*), the ventralizing activity of Pinhead was not obviously affected when a hemagglutinin (HA) epitope tag was fused to the carboxy end (Fig. 1D). Moreover, ectopic expression of *Xenopus pinhead* (NM_203534.1, NCBI) in zebrafish embryos generated similar ventralized phenotypes but did not result in macrocephaly (fig. S1, C and D), which had been observed in *pinhead*-overexpressed *Xenopus* embryos, suggesting an additional function of *pinhead* in the development of *Xenopus* nervous system (*22*).

In addition to the morphological changes, we also assessed the expression of several dorsal and ventral markers in embryos injected with 100 pg of *pinhead* mRNA. During the gastrula stages, injection of *pinhead* mRNA greatly reduced the expression of dorsal markers, including *chd* and *gsc* (Fig. 1, E and G). By contrast, the expression of the ventral markers *eve1* and *vent* was notably expanded in response to injection of *pinhead* mRNA (Fig. 1, F and G). In addition, embryos injected with *pinhead* mRNA had a much smaller dorsal neuroectoderm (as indicated by *sox3* expression), as well as an expanded ventral nonneural ectoderm (as indicated by *gata2* expression) at 75% epiboly stage (Fig. 1H). At later stages, overexpression of *pinhead* in zebrafish embryos resulted in a slight expansion of the blood cell population within the intermediate cell mass, which is derived from the ventral mesoderm (Fig. 1I). On the basis of these observations, we conclude that Pinhead has ventralizing functions in the zebrafish embryonic body plan.

The *pinhead* gene encodes a functional BMP ligand

Zebrafish *pinhead* encodes a 316–amino acid protein with a predicted hydrophobic N-terminal signal sequence (fig. S1E). Because Pinhead is a ventralizing factor and predicted to be secreted, we speculated that it is a BMP-like ligand. To address this hypothesis, we compared the sequences of Pinhead and several zebrafish BMP members, including BMP2b, BMP4, BMP7a, and Admp. Although the sequence

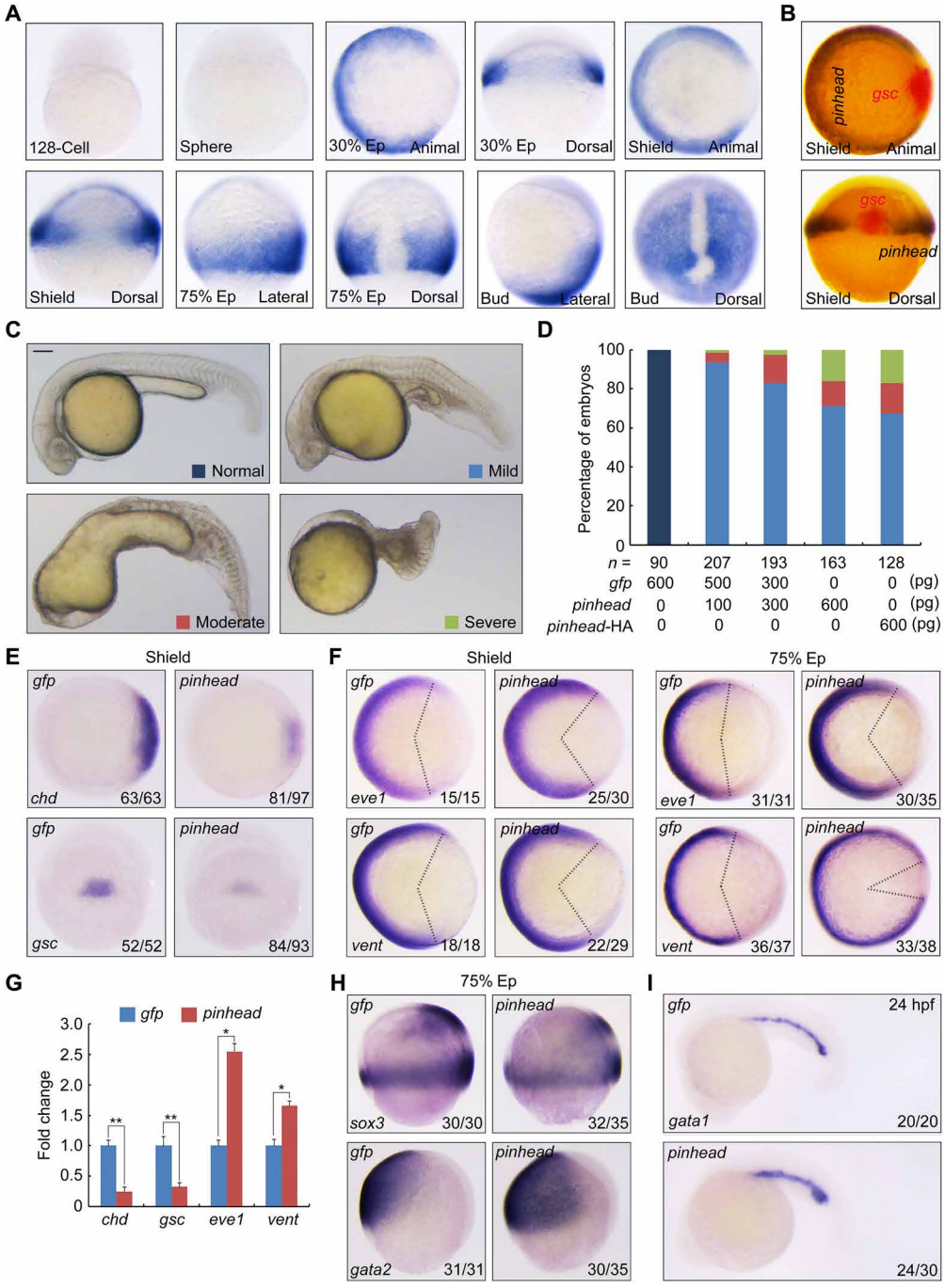

Fig. 1. Overexpression of *pinhead* ventralizes zebrafish embryos. (**A**) Expression of *pinhead* in wild-type zebrafish embryos was analyzed by whole-mount in situ hybridization. 128-Cell and sphere stages, lateral views; 30% epiboly (ep) and shield stages, animal pole views with dorsal to the right, and dorsal views with animal pole at the top; and 75% epiboly and bud stages, lateral views with dorsal to the right, and dorsal views with animal pole at the top. In the last panel, the embryo is slightly tilted upward to expose the tail bud. (**B**) Double in situ hybridization of *pinhead* (dark blue) and *gsc* (red) expression at the shield stage. In the upper panel, the animal pole view shows the relative positions of the *pinhead* and *gsc* domains. In the lower panel, the dorsal view displays *pinhead* and *gsc* transcripts in embryos at exclusive domains. (**C** and **D**) Embryos were injected with different doses of *gfp* or *pinhead* mRNAs. Representative pictures of different classes and statistical data are shown in (C) (lateral views with anterior to the left) and (D). Scale bar, 100 μm. (**E** and **F**) The expression of dorsal (E, *chd* and *gsc*) and ventral (F, *eve1* and *vent*) marker genes in *gfp* and *pinhead* mRNA–injected embryos at the indicated stages. (E) Animal views with dorsal side to the right in upper panels, and dorsal views with animal pole at the top in lower panels. (F) Animal views with dorsal to the right. (**G**) Expression levels of several dorsal-ventral genes were analyzed at the shield stage by real-time quantitative (qPCR). The expression levels of β-actin were used as a reference to normalize the amount of mRNAs in each sample. Error bars indicated SD. Asterisks indicated statistical significance of difference, $*P < 0.05$; $**P < 0.01$, Student's *t* test. (**H**) Analysis of the expression patterns of the dorsal neuroectoderm marker *sox3* and ventral nonneural ectoderm marker *gata2* at the 75% epiboly stage. Lateral views with the dorsal side pointing to the right. (**I**) The expression pattern of *gata1* in *gfp* and *pinhead* mRNA-injected embryos. Lateral views with anterior to the left.

of Pinhead displays little similarity to the other BMP ligands, it does contain a number of features characteristic of BMP proteins, including a consensus Arg-X-X-Arg proteolytic processing site and six characteristic cysteine residues conservatively located in the mature carboxyl terminal domain (fig. S1F).

To examine the biochemical properties of Pinhead, we expressed Pinhead-HA protein in human embryonic kidney (HEK) 293T cells and studied the conditioned medium produced by the transfected cells (Pinhead CM). Immunoprecipitation of Pinhead CM revealed that the Pinhead protein was present in the medium (Fig. 2A). To analyze the secretion rate of Pinhead, we treated HEK293T cells expressing Pinhead-HA with the protein synthesis inhibitor, cycloheximide (CHX), and then immunoprecipitated Pinhead proteins in conditioned medium and cell lysates at different time points, respectively. We found that about 30% of Pinhead proteins were secreted within 4 hours, and more than 90% of Pinhead proteins were present in the medium after 12 hours of CHX treatment (Fig. 2, B and C). In addition, after 8 hours of CHX treatment, we detected more than 90% of Pinhead proteins in the CM produced by the suspended cells dissociated from the gastrula embryos injected with *pinhead*-HA mRNA (fig. S1, G and H), suggesting that Pinhead proteins can be more effectively processed in and secreted from zebrafish embryonic cells.

To further demonstrate that Pinhead is a secreted protein in vivo, we examined whether Pinhead is secreted in zebrafish embryos by coinjecting mRNAs encoding plasma membrane–localized mCherry-CAAX protein and Pinhead-GFP protein, in which green fluorescent protein (GFP) was fused to the C-terminal end of Pinhead, into one-cell stage embryos. The Pinhead-GFP fusion protein has a ventralizing activity similar to untagged Pinhead, as injection of equimolar amounts of *pinhead-gfp* and *pinhead* mRNAs resulted in similar percentages of ventralized embryos at 24 hpf (fig. S1, I and J). As expected, Pinhead-GFP protein was primarily intercellular at the shield stage (Fig. 2D). We also injected *pinhead-gfp* mRNA together with rhodamine-dextran into one marginal blastomere at the 16- or 32-cell stages. At later stages, the descendant cells could be indicated by rhodamine fluorescence. At the shield stage, we observed obvious GFP fluorescence at the periphery of the rhodamine-positive and rhodamine-negative cells and even the cells far away from the progeny of the injected blastomere (Fig. 2E). Immunoprecipitation of CM produced by the suspended cells from embryos injected with *gfp* or *pinhead-gfp* mRNAs showed that it was not GFP protein but Pinhead-GFP that could be detected in the medium (fig. S1K), ruling out the possibility that the high mobility of the protein observed in zebrafish embryos is due to a substantial amount of free GFP. Thus, these results suggest an efficient secretion and a long-range diffusion of Pinhead proteins in the developing embryos.

The mature form of Pinhead is one conserved cysteine residue less than other BMP ligands (fig. S1F). Therefore, we next examined whether secreted Pinhead protein could form covalent dimers that had been proved to be essential for downstream signaling events (*3*). Pinhead-HA proteins were enriched from the CM by immunoprecipitations and then subsequently separated on reducing and nonreducing SDS–polyacrylamide gel electrophoresis (PAGE), respectively. Immunoblotting analysis showed a single SDS-resistant band with an apparent molecular weight of about 70 kDa under nonreducing conditions, which migrated much more quickly under reducing conditions (Fig. 2F), implicating that most of the mature Pinhead proteins exist as disulfide-linked dimers in vivo. To determine whether secreted Pinhead activates an intracellular signaling cascade, we measured the phosphorylation levels of Smad1/5/8 in Hep3B cells in the presence and absence of Pinhead CM. We found that stimulation with recombinant BMP4 or Pinhead CM substantially enhanced Smad1/5/8 phosphorylation, and combining BMP4 and Pinhead CM further promoted this phosphorylation (Fig. 2G). By contrast, Smad2 phosphorylation (p-Smad2) in Hep3B cells was induced by incubations with TGF-β1 but not Pinhead CM (Fig. 2H). In addition, overexpression of *pinhead* in embryos had no effects on p-Smad2 expression (Fig. 2H). These data not only demonstrate that Pinhead specifically triggers the BMP pathway but also rule out the possibility that Pinhead ventralizes embryos by inhibiting Nodal signaling, which is required for the formation of the organizer and the dorsal axial structures. Moreover, Pinhead binds to and signals through BMP receptors, as Pinhead CM–induced Smad1/5/8 phosphorylation was totally abolished in the presence of the selective BMP type I receptor inhibitor dorsomorphin or DMH1, and overexpressed Pinhead was coimmunoprecipitated with BMP type I receptors ALK2, ALK3, ALK6, and ALK8 (Fig. 2, I and J). We were not expecting to find an association between Pinhead and TGF-β type I receptor ALK5 (Fig. 2J). However, this Pinhead-ALK5 association may not have biological significance, as Pinhead proteins did not induce phosphorylation of Smad2 in Hep3B cells and zebrafish embryos (Fig. 2H).

In zebrafish embryos, injection of 100 pg of *pinhead*-HA mRNA promoted phosphorylation of Smad1/5/8 during gastrulation (Fig. 2K). Pinhead protein efficiently coimmunoprecipitated with the BMP antagonist Chd and Noggin1 (Fig. 2, L and M). The *pinhead* overexpression–induced DV defects in the shield-stage embryos, such as the reduction in *gsc* expression and the expansion of *eve1* expression, were eliminated by coinjecting 10 pg of *chd* mRNA (Fig. 2, N and O). Consistent with these observations, at 24 hpf, injection of *chd* mRNA well rescued the ventralized morphology in Pinhead-overexpressing embryos (fig. S1L). Together, these findings indicate that Pinhead is a functional BMP ligand during zebrafish embryo development.

The *pinhead* and *admp* genes repress one another and compensatorily function in DV patterning

To examine the in vivo functions of *pinhead*, we generated a *pinhead* mutant by targeting exon 1 with the CRISPR-Cas9 system. The mutant was named *ph*Δ49, as there was a 49–base pair (bp) deletion that led to the loss of the translational start site (fig. S2A). We further generated the maternal-zygotic mutant by incrossing homozygous *pinhead* zygotic mutants. In situ hybridization experiments revealed an obvious decrease in *pinhead* transcripts in the *phΔ49* mutants, providing further evidence that this mutant is a null allele of the *pinhead* gene (fig. S2B). Unexpectedly, *ph*Δ49 embryos had normal morphologies at the end of gastrulation and at 24 hpf (fig. S2, C and D). In addition, we found no DV pattern defects in *phΔ49* mutants for typically expressed dorsal and ventral genes (fig. S2, E and F). Previous studies indicate that a compensatory network may be activated to buffer against deleterious mutations, which was not observed after translational or transcriptional knockdown (*25*). Therefore, knockdown experiments were performed using an antisense MO (*ph* MO) that interfered with translation by targeting the *pinhead* sequence and efficiently blocking the production of the Pinhead-GFP fusion protein in embryos (fig. S2G). However, injection of 5 ng of *ph* MO into wild-type embryos did not result in any obvious DV defects (fig. S2, H and I). Therefore, the loss of *pinhead* does

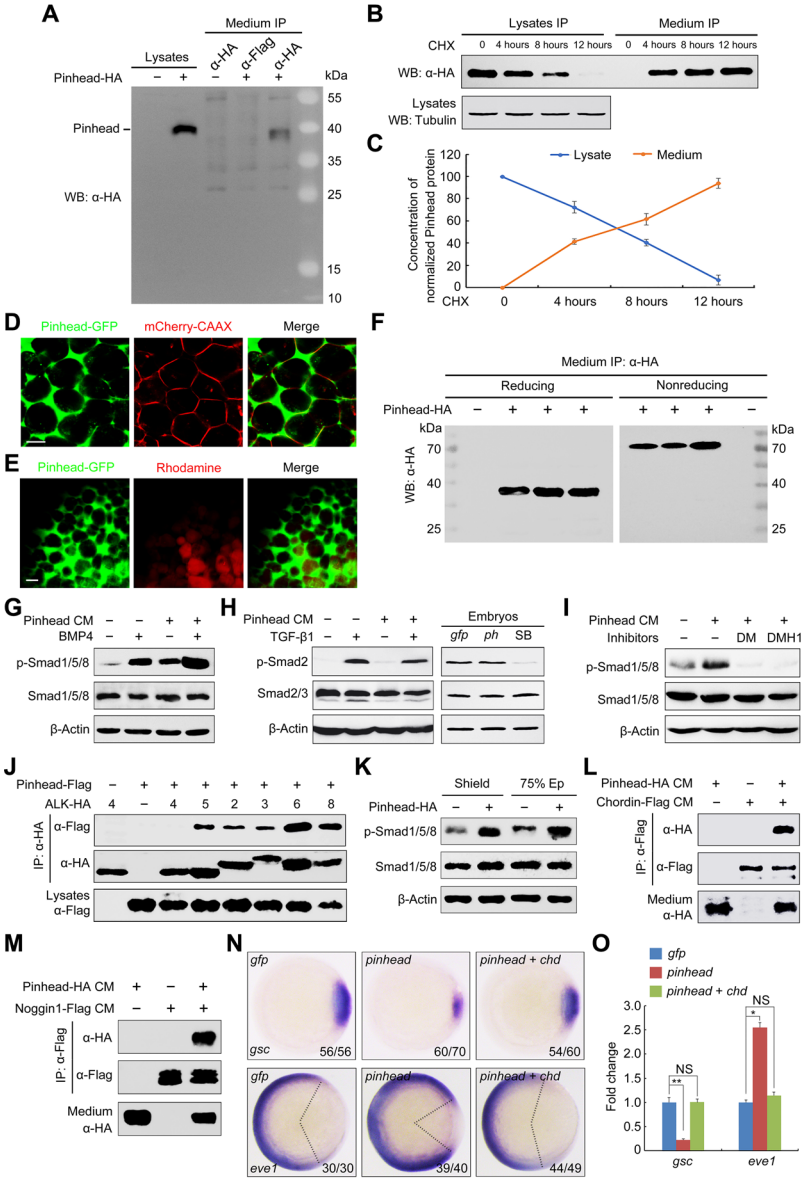

Fig. 2. Pinhead is a secreted functional BMP ligand. (**A**) The CM from HEK293T cells transfected with Pinhead-HA was examined using an immunoprecipitation assay. Pinhead levels in cell lysate were examined by Western blot as a positive control. Underlying data can be found in data file S1. (**B** and **C**) HEK293T cells were transfected with Pinhead-HA plasmids. Twenty-four hours later, cells were treated with CHX (20 μg/ml) for the indicated times. Then, the CM and CHX-treated cells were harvested for immunoblotting (B). Pinhead-HA protein levels were quantified and normalized to tubulin (mean ± SD, three independent biological repeats; C). Underlying data can be found in data file S1. (**D** and **E**) Pinhead-GFP fusion proteins were efficiently secreted from zebrafish embryonic cells. In (D), 50 pg of *pinhead*-GFP mRNA and 50 pg of mCherry-CAAX mRNA were coinjected into embryos at the one-cell stage. In (E), 10 pg of *pinhead*-GFP mRNA together with rhodamine-dextran was injected into one marginal blastomere at the 16- or 32-cell stage. All embryos were imaged using a Nikon A1R+ confocal microscope at the shield stage. Scale bar, 10 μm. (**F**) Pinhead-HA proteins were enriched from the CM by immunoprecipitation and then subsequently separated on reducing and nonreducing SDS-PAGE. Underlying data can be found in data file S1. (**G** and **H**) Hep3B cells were treated with Pinhead CM alone or together with BMP4 (G) or TGF-β1 (H) for 1 hour and then harvested for Western blots with the indicated antibodies. The expression of β-actin was analyzed as a loading control. In (H), wild-type embryos treated with 25 μM SB431542 (SB) from the 16-cell stage and embryos injected with 100 pg of *gfp* or *pinhead* mRNA at the one-cell stage were also harvested at the shield stage and subjected to immunoblotting. Underlying data can be found in data file S1. (**I**) Hep3B cells were treated with Pinhead CM alone or together with the indicated BMP type I receptor inhibitors for 4 hours and then harvested for Western blot with the indicated antibodies. Note that Pinhead CM-induced Smad1/5/8 phosphorylation notably decreased in the presence of BMP type I receptor inhibitors. Underlying data can be found in data file S1. (**J**) Pinhead binds to BMP type I receptors. HEK293T cells were transfected as indicated with expression plasmids encoding Flag-tagged Pinhead and HA-tagged BMP type I receptors and harvested for immunoprecipitation with an anti-HA antibody. Underlying data can be found in data file S1. (**K**) Western blots of total lysates from embryos injected with 100 pg of *pinhead*-HA mRNA. Underlying data can be found in data file S1. (**L** and **M**) Extracellular Pinhead interacts with Chd (L) and Noggin (M). CM were prepared from HEK293T cells transfected with indicated plasmids. Immunoprecipitation assays were performed using an anti-Flag antibody. Underlying data can be found in data file S1. (**N**) Overexpression of *chd* rescues Pinhead-induced DV defects. Embryos were injected with 100 pg of *pinhead* mRNA alone or together with 10 pg of *chd* mRNA at the one-cell stage and collected at the shield stage for in situ hybridization. (**O**) Expression levels of *gsc* and *eve1* were analyzed at the shield stage by real-time qPCR. Error bars indicated SD. *$P < 0.05$; **$P < 0.01$, Student's *t* test. NS, not significant.

not disturb the formation of the DV axis, and an additional signal may be present in the embryo to compensate for the lack of *pinhead*.

The genes *pinhead* and the BMP ligand-encoding *admp* exist in tandem in the genomes of various animals, including zebrafish. These two genes have diametrically opposed expression patterns in the trunk epidermis in gastrulating *Ciona* embryos (*23*). We speculate that *admp* is an ideal candidate for buffering the loss of *pinhead*. In support of this hypothesis, contrary to the narrowed expression of *admp* in *pinhead*-deficient *Ciona* embryos (*23*), we found *admp* expression to be up-regulated in zebrafish *phΔ49* mutants at the 30% epiboly and shield stages (Fig. 3A). To exclude the possibility that the increase in *admp* expression was merely an adaptation for gene loss, we injected 5 ng of *ph* MO into wild-type embryos. We found that *admp* expression also greatly increased in the *pinhead* morphants (Fig. 3B), suggesting that *admp* expression is repressed by *pinhead*. We also generated a null allele of *admp* with an 11-bp deletion in exon 1 (*adΔ11*) (fig. S3, A and B). Mild dorsalization phenotypes were observed in knockdown experiments with *admp* MO in *Xenopus* and zebrafish (*8*, *12*, *16*, *17*). By contrast, the morphology and DV polarity were not affected in *adΔ11* maternal-zygotic mutants compared to the wild-type control (fig. S3, C to F). It had been reported that *admp* morphants exhibited a notable enlargement of *gsc* expression domain and an evident diminution of *eve1* expression (*14*). Unexpectedly, we did not observe any marked changes in the expression of dorsal-ventral markers in embryos injected with 3 ng of *admp* MO (fig. S3, G and H), which had previously been used (*14*). This inconsistency may be due to the different experimental conditions between the studies. *pinhead* expression was evidently expanded in *adΔ11* mutants and *admp* morphants (Fig. 3, C and D). These results reveal that *pinhead* and *admp* are expressed in a "seesaw"-like fashion through opposing transcriptional regulation in the embryonic body plan.

As shown in Fig. 3E, coimmunoprecipitation experiments revealed a steady binding of secreted Pinhead and Bamp1a, a Xolloid-related metalloproteinase that plays a pivotal role in proteolytic cleavage of Chd in zebrafish (*26*). The association of Pinhead with Bamp1a led us to examine whether Pinhead regulates BMP1a-mediated Chd degradation. Compared with the effects of the corresponding untagged proteins, overexpression of Admp-HA or Chd-Flag in wild-type embryos caused similar or slightly alleviated DV polarity defects at 24 hpf (fig. S4, A to D), suggesting that the addition of C-terminal epitopes has no obvious impact on their activities. Then, BMP1a, Chd, Admp, and Pinhead proteins were prepared by collecting the corresponding CM produced by transfected HEK293T cells. When BMP1a was coincubated with Chd, we detected a decrease in Chd protein, where adding Admp further facilitated this cleavage (Fig. 3F), suggesting that the secreted BMP1a functions well in our biochemical system. Pinhead was then coincubated with BMP1a and Chd in vitro, which promoted a reduction in Chd levels (Fig. 3G). These observations demonstrate that, similar to Admp, Pinhead promotes metalloproteinase-mediated Chd degradation.

To further confirm the roles of *pinhead* and *admp* in the formation of DV polarity in zebrafish embryos, we deleted the *pinhead* gene in the *adΔ11* mutants using the CRISPR-Cas9 system. One mutant was obtained with an identical 49-bp deletion in the *pinhead* gene in the *adΔ11* background. The $phΔ49^{+/-};adΔ11^{-/-}$ embryos develop normally and are viable and fertile, but $phΔ49^{-/-};adΔ11^{-/-}$ embryos began to die 36 hpf, with a few surviving up to adulthood. Homozygous *pinhead* and *admp* double-mutant embryos were generated by crossing the surviving adults. Most of the *phΔ49;adΔ11* double mutants had an ovoid shape at the bud stage and a clearly shortened posterior trunk and reduced yolk extension at 24 hpf, all of which are characteristic of dorsalization (Fig. 3, H and I). Furthermore, although injection of *pinhead* MO or *admp* MO into wild-type embryos did not lead to observable DV polarity defects at 24 hpf, coinjection of these MOs generated a dorsalized phenotype very similar to that of *phΔ49;adΔ11* double mutants (fig. S5A), excluding the potential CRISPR-Cas9 off-target effects.

The dorsalization phenotypes in *phΔ49;adΔ11* double mutants were further confirmed by the expression of several dorsal and ventral markers. As shown in Fig. 3J, we observed a marked expansion in the dorsal markers *chd* and *gsc* in *phΔ49;adΔ11* embryos, while the expression of these markers remained unchanged in the *phΔ49* and *adΔ11* single mutants compared to the wild-type embryos. Meanwhile, the expression of the ventral marker *eve1* was nearly abolished in *phΔ49;adΔ11* embryos (Fig. 3K). Genetic deletion of these two genes consistently caused enlargement of dorsal-related tissues, including the prechordal plate (indicated by *gsc*) and notochord (indicated by *ntl*) (fig. S5B). There was also a large decrease in the blood cells located in the intermediate cell mass in *phΔ49/adΔ11* mutants (fig. S5C). It has been reported that dorsalized embryos exhibit a slightly widened adaxial domain and expanded somite due to loss of *swirl/bmp2b* (*11*, *24*). However, *phΔ49/adΔ11* mutants showed reduced presomitic mesoderm (indicated by *papc*) at the bud stage (fig. S5D), which might reflect a role of *pinhead* and *admp* in somitogenesis, as *pinhead* transcripts were highly enriched in the presomitic mesoderm at the end of gastrulation (Fig. 1A). In addition, at the shield stage, phosphorylation of Smad proteins and the BMP gradient decreased in the *phΔ49/adΔ11* embryos (Fig. 3, L and M). Consistent with previous reports that *bmp* expression is maintained through autoregulatory feedback loops (*24*, *27*), we observed that, compared to the wild-type embryos at the shield stage, *phΔ49;adΔ11* double mutants displayed reduced expression of *bmp2b*, *bmp4*, and *bmp7a*, which were not obviously changed in *phΔ49* and *adΔ11* single mutants (fig. S5E). In addition, by knockdown of *admp* in *phΔ49* mutants or injection of *pinhead* MO into *adΔ11* embryos, we observed similar dorsalization phenotypes, including the changes in the expression of dorsal and ventral markers (fig. S6, A to D), the repression of Smad1/5/8 phosphorylation (fig. S6, E and F), and the destruction of the BMP activity gradient (fig. S6, G and H). These results further confirm that *pinhead* and *admp* function together to regulate the formation of the BMP activity gradient and DV patterning in early zebrafish embryos.

It is well established that Admp functions in DV axis formation by enhancing Chd degradation (*12*, *15*). Moreover, Admp overexpression could enhance the ventralized phenotype of *din* homozygous mutants, a mutant allele of *chd* (*28*), suggesting a role for Admp in BMP signal activation through a Chd-independent manner. It has been proved that Admp has BMP-like activity and signals via the ALK2 receptor (*8*). Given that Pinhead has similar functional properties to Admp, we asked whether Pinhead functions as a secreted scaffold aiding in Chd degradation and a ligand involved in activating BMP signaling during zebrafish DV patterning. We first examined the expression levels of endogenous Chd in shield-stage *phΔ49* and *adΔ11* mutants by Western blot analysis using a previously validated antibody (*17*). We found that the endogenous Chd protein heavily accumulated in *phΔ49;adΔ11* double mutants compared to wild-type or single-mutant embryos (fig. S7A). In contrast, the expression of Chd

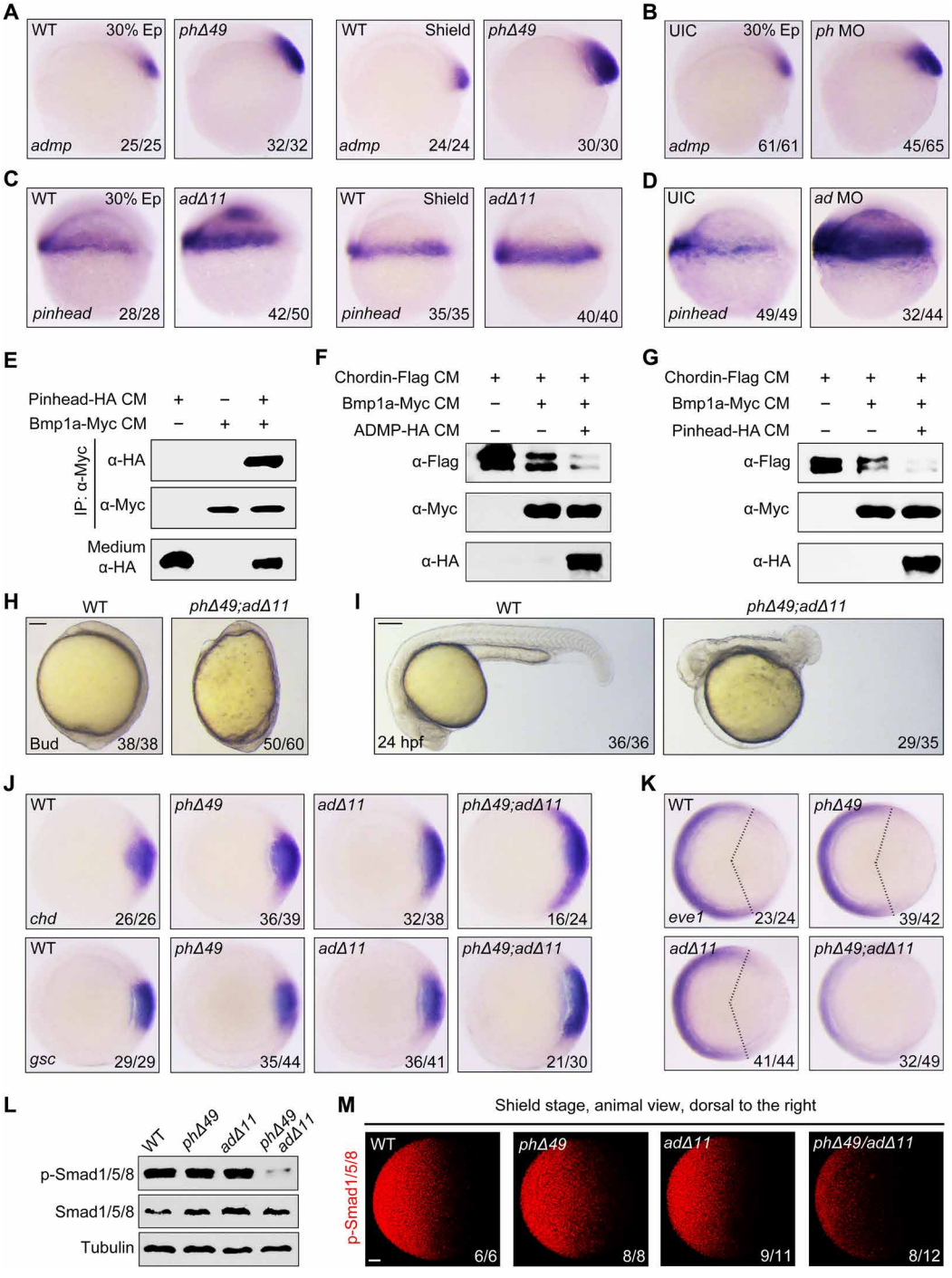

Fig. 3. Pinhead and Admp repress one another and compensatorily function in DV patterning. (**A** and **B**) The expression pattern of *admp* in wild-type, *pinheadΔ49* homozygous mutant, and 5-ng *pinhead* MO (*ph* MO)–injected embryos at the indicated stages. (**C** and **D**) The expression pattern of *pinhead* in wild-type, *admpΔ11* homozygous mutant, and 3-ng *admp* MO (*ad* MO)–injected embryos at the indicated stages. (**E**) Pinhead binds to BMP1a. HEK293T cell-produced Pinhead-HA was coincubated with or without BMP1a-Myc–containing medium at 4°C for 12 hours. The interactions between Pinhead and BMP1a were analyzed with an anti-HA antibody. Underlying data can be found in data file S1. (**F** and **G**) Admp or Pinhead promotes BMP1a-mediated Chd degradation. HEK293T cell–produced Chd-Flag protein was incubated with the indicated CM at 4°C for 12 hours, and then analyzed by Western blot with an anti-Flag antibody. Underlying data can be found in data file S1. (**H** and **I**) Morphological defects in *phΔ49;adΔ11* double-mutant embryos. Note the ovoid shape at the bud stage (H) and the shortened posterior trunk at 24 hpf (I) in *phΔ49;adΔ11* double mutants. Scale bar, 100 μm. (**J** and **K**) The expression patterns of dorsal and ventral markers in wild-type and indicated mutant embryos. Note that the double depletion of *pinhead* and *admp* results in evidently increased expression of dorsal markers *chd* and *gsc* (J) and reduced expression of ventral marker *eve1* (K) at the shield stage. (**L** and **M**) Wild-type and indicated mutant embryos were harvested at the shield stage for Western blots (L) and immunofluorescence assays (M) with the indicated antibodies. Note the distinct decrease in Smad1/5/8 phosphorylation in the *phΔ49/adΔ11* double mutants. Scale bar, 50 μm. Underlying data can be found in data file S1.

evidently decreased upon injection of *pinhead* or *admp* mRNA (fig. S7B). To avoid the influence of changes in endogenous Chd expression induced by DV defects, we further examined the expression of exogenous Chd-HA protein in *phΔ49;adΔ11* double mutants and wild-type embryos. All the embryos were injected with the same amount of *chd*-HA mRNA (50 pg) at the one-cell stage. Western blot results showed that the expression level of Chd-HA was up- or down-regulated upon depletion or overexpression of *pinhead/admp* (fig. S7, C and D). These results indicate that Pinhead can facilitate Chd degradation in vivo.

We next tested whether Pinhead also has a role in DV patterning when *chd* and *bmp2b* are depleted. As previously reported, injection of *bmp2b* MO into wild-type embryos caused a severe dorsalized morphology at 24 hpf, while the interference with *chd* function by MO generated a clear ventralized phenotype (fig. S7E) (*29*, *30*). As expected, double depletion of *chd* and *bmp2b* gave a nearly normal morphology (fig. S7E). Injection of 100 pg of *pinhead* mRNA into *chd/bmp2b*-depleted embryos led to a ventralized phenotype, which was slightly serious in embryos injected with the same amount of *admp* mRNA (fig. S7E). Thus, similar to Admp, Pinhead might also regulate the establishment of DV regionalization via its BMP-like activity.

On the basis of these results, overexpression of either *pinhead* or *admp* would be expected to compensate for the loss of these two genes. Injection of 5 pg of *bmp2b* mRNA into the *phΔ49;adΔ11* mutant embryos efficiently reversed the dorsalization morphologies (fig. S7F). Injection of either 100 pg of *pinhead* mRNA or 50 pg of *admp* mRNA also considerably alleviated the DV defects in the *phΔ49;adΔ11* mutants (fig. S7F). Thus, the consistency in the molecular nature and the opposite transcriptional regulation of Pinhead and Admp provides an important compensatory mechanism by which to maintain stability of axial patterning when one of these genes is disrupted.

BMP signaling negatively regulates *pinhead* and *admp* expression

In *Ciona* gastrulas, *pinhead* is expressed in the posterior ventral epidermal cells, while *admp* is expressed in the dorsal epidermis. Their mutually exclusive expression is regulated at the chromatin level by a *cis*-acting mechanism that is widely conserved between animals (*23*). When the *cis*-acting repression is relieved, ectopic *admp* expression is observed in the ventral region (*23*). Expression of *admp* greatly increased in the *phΔ49* mutant but did not spread into the ventrolateral regions, suggesting that the microdeletion in the *phΔ49* mutant did not alter the chromosomal conformation around the gene locus (Fig. 3, A and B). Repression of *admp* by BMP signaling and the BMP-like activity of Pinhead prompted us to examine whether the up-regulation in *admp* expression in the *phΔ49* mutants was due to a transient decline in BMP signaling induced by Pinhead deficiency.

As shown in Fig. 4 (A and B), wild-type embryos injected with *bmp2b* MO or treated with the BMP inhibitor dorsomorphin or DMH1 had remarkably increased expression of *admp*. Conversely, injection of *bmp2b* mRNA led to a reduction in a*dmp* expression (Fig. 4, C and E). In addition, the expression of *pinhead* was negatively regulated by BMP signaling, as knockdown of *bmp2b* induced and high levels of *bmp2b* inhibited its transcription (Fig. 4, A, B, D, and E). The increased expression of *admp* and *pinhead* in the corresponding mutants was reduced to a lower level than that in wild-type embryos by injection of 10 pg of *bmp2b* mRNA (Fig. 4, F to H), indicating a complete compression of the compensatory expression of *pinhead* or *admp* upon BMP2b overexpression. Therefore, we conclude that BMP signals negatively regulate *pinhead* and *admp* transcription. In addition, wild-type embryos injected with 10 pg of *bmp2b* mRNA displayed various ventralized phenotypes ranging from mild to severe at 24 hpf (fig. S8, A and B). Upon *bmp2b* mRNA injection, the *phΔ49* and *adΔ11* single mutants exhibited a similar ventralized morphology (fig. S8, A and B), further suggesting that the compensatory expression of *pinhead* or *admp* can make up for the gene loss in the corresponding mutants.

On the basis of the "seesaw"-like expression patterns of *pinhead* and *admp*, we speculate that, when the expression of one is disturbed in embryos, BMP signaling will temporarily be lower and expression of the other gene will be subsequently promoted to support the self-regulation of the BMP signaling levels for the embryonic body plan. To address this issue, MOs targeting *pinhead* or *admp* were injected into *Tg(BRE:EGFP)* embryos, in which a GFP reporter can reveal the dynamic changes in BMP activity during embryonic development (*31*). In support of our hypothesis, the results of real-time quantitative polymerase chain reaction (PCR) analysis revealed an early partial loss of BMP activity in the morphants, which was dynamically compensated before the shield stage (Fig. 4I). The expression of *admp* in *phΔ49* mutants or *pinhead* in *adΔ11* mutants was gradually elevated compared to that in wild-type embryos (Fig. 4, J and K). The promotion of *admp* and *pinhead* expression may well be due to the temporary reduction in BMP activity in the single-mutant embryos, as coinjection of 10 pg of *bmp2b* mRNA notably suppressed the elevation of their expression (Fig. 4, J and K).

Smad proteins directly bind to *pinhead* and *admp* enhancers

To further investigate whether BMP/Smad signaling directly represses *pinhead* and *admp* transcription, we amplified 1336 bp of the *admp* and 1516 bp of the *pinhead* promoter regions upstream of the translation start site of each gene and fused them to GFP cDNA to create reporter constructs (named −1336-*ad*-P-GFP and −1516-*ph*-P-GFP, respectively). The upstream sequence of *admp* drove GFP expression on the dorsal side of shield stage embryos, recapitulating endogenous expression of *admp* (Fig. 5A). Next, we generated serial truncations of the *admp* promoter and injected them into embryos. We found that the truncated promoter containing the −633-bp upstream sequence (−633-*ad*-P-GFP) exhibited transcriptional activity in the dorsal region similar to the full-length promoter, while the −210-*ad*-P-GFP construct lost the ability to express GFP (Fig. 5A), suggesting that the region between −633 and −210 bp is an enhancer essential for *admp* expression. To identify potential BMP/Smad-responsive elements in this enhancer, we injected the −633-*ad*-P-GFP construct (100 pg) into wild-type and *phΔ49* mutant embryos. The expression of −633-*ad*-P-GFP was augmented in DMH1-treated wild-type and *phΔ49* mutant embryos (Fig. 5B), suggesting that the enhancer responds well to BMP signals. To quantitatively analyze the transcriptional regulation of *admp* by BMP signal, we generated a luciferase reporter plasmid (−633-*ad*-P-Luc) by subcloning the −633-bp upstream sequence of *admp* into pGL3-Basic vector. As expected, 3- or 4.5-fold enhanced transcriptional activity of −633-*ad*-P-Luc was observed in *pinhead* defective or DMH1-treated embryos (Fig. 5C). Similarly, a BMP signal-responsive enhancer that specifically drove reporter gene expression in the ventral and lateral margin of the gastrulas was identified between −431 and −225 bp in the *pinhead* promoter (Fig. 5, D to F).

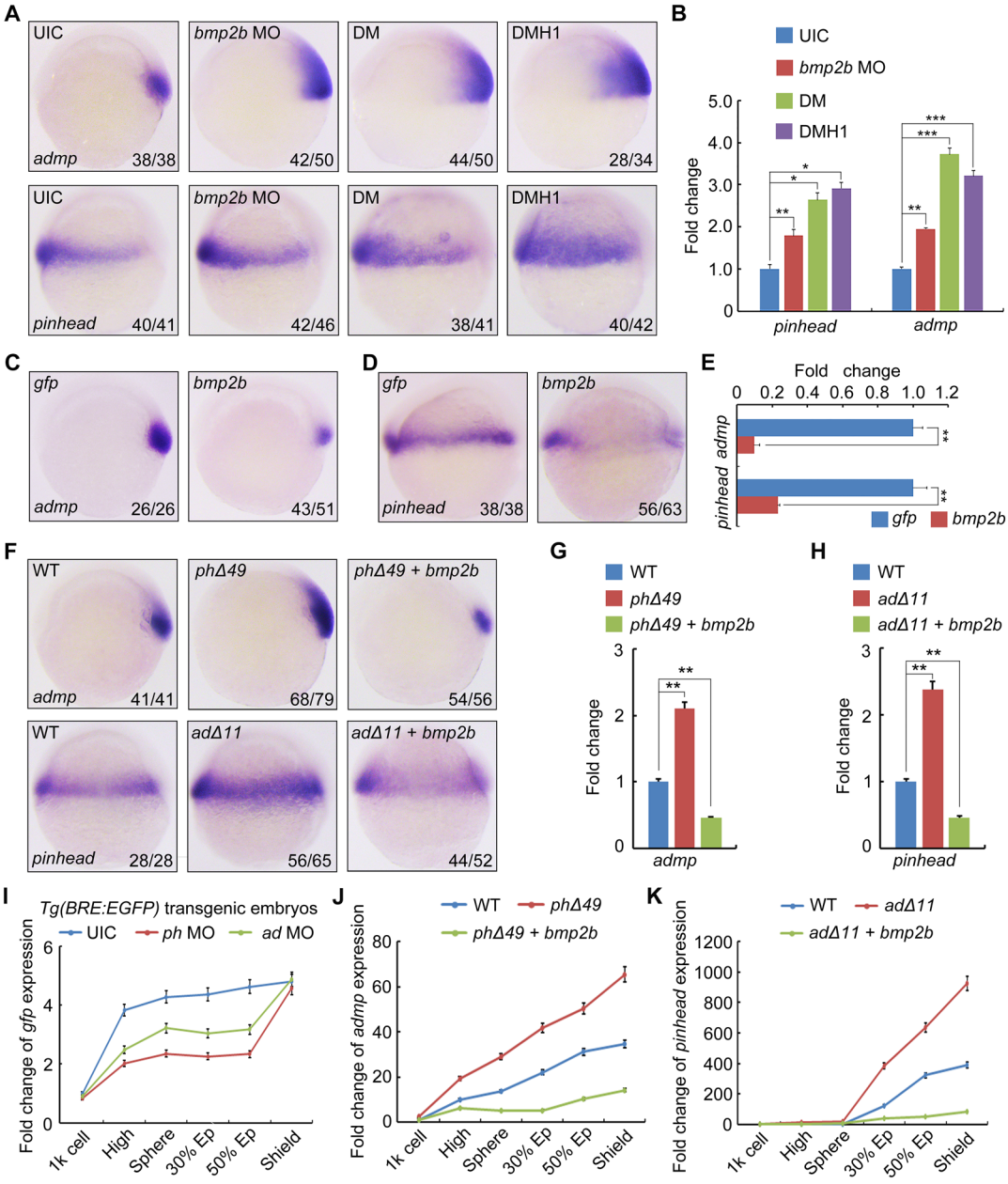

Fig. 4. Expression of *pinhead* and *admp* is repressed by BMP signaling. (**A** and **B**) The expression of *admp* and *pinhead* was analyzed at the shield stage by in situ hybridization (A) and real-time qPCR in *bmp2b* morphants and embryos treated with 10 μM dorsomorphin or 5 μM DMH1 from the 1K cell stage. Error bars indicated SD. **P* < 0.05; ***P* < 0.01; ****P* < 0.001, Student's *t* test. UIC, uninjected control. (**C** and **D**) The expression of *admp* and *pinhead* was obviously decreased at the shield stage in embryos injected with 10 pg of *bmp2b* mRNA. (**E**) Embryos injected with 10 pg of *bmp2b* mRNA were harvested for real-time qPCR analysis. ***P* < 0.01, Student's *t* test. (**F** to **H**) Overexpression of *bmp2b* inhibited the expansion of *admp* expression in *phΔ49* mutants and *pinhead* expression in *admpΔ11* mutants. *phΔ49* and *admpΔ11* mutant embryos were injected with 10 pg of *bmp2b* mRNA at the one-cell stage and harvested at the shield stage for in situ hybridization (F). The expression of *admp* and *pinhead* was also analyzed by real-time qPCR (G and H). Error bars indicated SD. ***P* < 0.01, Student's *t* test. (**I**) The self-regulation of the BMP signaling levels in *pinhead*- or *admp*-depleted embryos. *Tg(BRE:EGFP)* transgenic embryos were injected with 5 ng of *pinhead* MO or 3 ng of *admp* MO at the one-cell stage and then harvested at indicated developmental stages for examination of *gfp* expression by real-time qPCR analyses. The expression of β-actin was used as an internal control. Error bars indicated SD. (**J** and **K**) The dynamics of *admp* (J) or *pinhead* (K) expression in indicated mutants injected with or without 10 pg of *bmp2b* mRNA. The expression levels of *admp* and *pinhead* were individually examined by real-time qPCR at the indicated stages, and the expression levels of β-actin were used as a reference to normalize the amount of mRNAs in each sample.

Smad proteins physically interact with the promoters of their target genes to regulate gene expression (*18*). Specifically, Smad1/5 proteins, the intracellular downstream mediators of BMP signaling, directly bind to the GC-rich elements in BMP/Smad target promoters (*32*). There are two and four potential Smad1/5-bound GC-rich elements in the *admp* and *pinhead* enhancers, respectively (fig. S9,

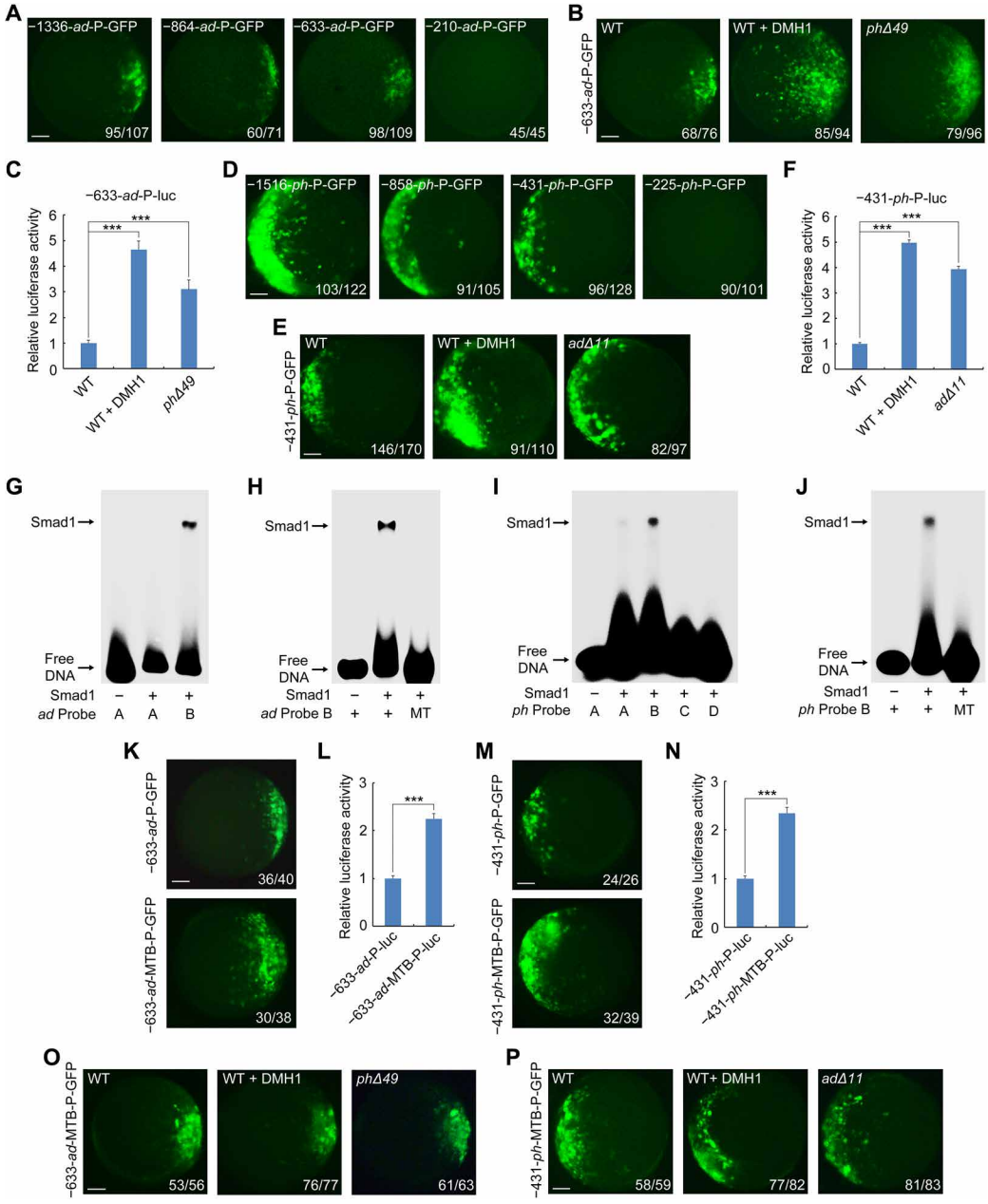

Fig. 5. Smad1 binds to and suppresses the enhancers of *pinhead* and *admp*. (**A**) The −633- to −210-bp region of the *admp* promoter was an important enhancer driving GFP expression in the dorsal side. Wild-type embryos were injected with various constructs as indicated at the one-cell stage and photographed at the shield stage. Animal pole views with dorsal to the right. Scale bar, 100 μm. (**B** and **C**) Responses of the *admp* enhancer to BMP signal inhibition. Wild-type and *phΔ49* mutant embryos were injected with 100 pg of the −633-*ad*-P-GFP (B) or −633-*ad*-P-luc (C) reporter construct at the one-cell stage and treated with or without 5 μM DMH1 from the 1K cell stage to the shield stage. Scale bar, 100 μm. ***$P < 0.001$, Student's *t* test. (**D** and **E**) Ventral and lateral margin expression of the *pinhead* promoter was determined by an enhancer located between −431- and −225-bp upstream of the transcription start site (D), which was heightened at the shield stage in *adΔ11* mutant and wild-type embryos treated with DMH1 (E). Animal pole views with dorsal to the right. Scale bar, 100 μm. (**F**) The expression of -431-*ph*-P-luc in indicated embryos was examined by luciferase measurement. The relative luciferase activity in each sample was the mean with SD from three independent experiments. ***$P < 0.001$, Student's *t* test. (**G** and **H**) Purified Smad1 bound specifically to *admp* probe B (*ad* Probe B) (G) and mutations in probe B abolished Smad binding (H). DNA-protein complexes were analyzed with a polyacrylamide gel and visualized by Typhoon FLA9500 Scanner. (**I** and **J**) Purified Smad1 directly bound to the wild-type *pinhead* probe B (*ph* Probe B) (G) but not the mutated probe (H). Electrophoretic mobility shift assays were performed similarly as in (G) and (H). (**K** to **N**) The mutated promoter reporters (−633-*ad*-MTB-GFP, −633-*ad*-MTB-luc, −431-*ph*-MTB-GFP, and −431-*ph*-MTB-luc) showed a higher transcriptional activity than the corresponding wild-type reporter. Wild-type embryos were injected with 100 pg of indicated reporter constructs at the one-cell stage. At the shield stage, these embryos were photographed (K and M) or subjected to luciferase assays (L and N). Scale bar, 100 μm. ***$P < 0.001$, Student's *t* test. (**O** and **P**) Smad binding was essential for BMP signal–mediated suppression of *admp* (O) and *pinhead* (P) transcription. Mutated reporter constructs (50 pg) were injected into wild-type and indicated mutant embryos at the one-cell stage, respectively. Wild-type embryos injected with −633-*ad*-MTB-GFP or −431-*ph*-MTB-GFP reporter were treated with or without DMH1 from the 1K cell stage. Note that these mutated reporters lost their ability to respond to BMP inhibition. Scale bar, 100 μm.

A and B). To explore the ability of Smad proteins to bind to these sites, we performed electrophoretic mobility shift assays using purified Smad1 proteins and synthesized probes containing presumptive Smad-binding sites. Smad1 specifically bound to *admp* probe B (*ad* Probe B) but not to the mutated probe with the "GGCGCC" to "AAAAAA" substitutions within the putative Smad1/5-binding site (Fig. 5, G and H, and fig. S9A). Meanwhile, Smad1 also bound to *pinhead* probe B (*ph* Probe B) but not its mutant (Fig. 5, I and J, and fig. S9B). When the proper mutations were introduced into each enhancer, the mutated promoters (100 pg of each) exhibited a remarkable increase of their transcriptional activities in wild-type embryos (Fig. 5, K to N), indicating a relief of direct repression by BMP/Smad signaling. Because the mutated promoters could activate much higher expression of reporter gene than their original promoters, we reduced the injection dosage to 50 pg to confirm whether they lose the ability to respond to BMP inhibition. We found that the GFP reporter driven by the mutated promoters was similarly expressed in DMH1-treated or untreated wild-type embryos and *phΔ49 or adΔ11* mutants (Fig. 5, O and P). Together, these results demonstrate that Smad1/5 binds to the *pinhead* and *admp* enhancers to repress their transcription in response to BMP signaling.

The *pinhead* and *admp* genes provide a dual protection system for the robustness of embryonic patterning

Embryonic DV patterning displays substantial resistance to experimental perturbations and Admp has been proposed to aid in the self-regulation of the BMP signaling gradient and the regeneration of normal DV structures (*8*, *12*). Because *pinhead* and *admp* are expressed under feedback regulations in a "seesaw"-like fashion and have compensatory functions in DV patterning, we presumed that both of these genes might be involved in the robust stability of axial patterning through fine-tuning of BMP signaling. To investigate whether *pinhead* and *admp* contribute to the buffering of BMP activity profiles against variations in gene dosage, we introduced *bmp2b* MO into *phΔ49 or adΔ11* mutants and *phΔ49;adΔ11* embryos injected with a rescuing amount of *pinhead* mRNA (improved *phΔ49;adΔ11* mutants). As shown in Fig. 6A, injection of 1 ng of *bmp2b* MO induced a mild increase of *chd* expression in most wild-type, *phΔ49,* and *adΔ11* embryos and caused a much stronger expansion of this dorsal marker gene in nearly 70% of the improved *phΔ49;adΔ11* mutants, where the DV defects were significantly rescued by *pinhead* overexpression (Fig. 6, A and B). In response to *bmp2b* MO injection, the expression domain of *chd* even extended to the ventral regions in about 20% improved *phΔ49/adΔ11* mutants, suggesting a much severe dorsalized phenotype (Fig. 6, A and B). Consistent with this, injection of 1 ng of *bmp2b* MO caused a more severe decrease in expression of the ventral marker *eve1* in improved *phΔ49;adΔ11* mutants compared to the control embryos (Fig. 6, A and C). These *bmp2b* morphants displayed different dorsalized morphologies (C1 to C5) at 24 hpf (Fig. 6, D and E). About 80% of the improved *phΔ49;adΔ11* embryos showed a normal DV morphology (Fig. 6E). Upon injection of 1 ng of *bmp2b* MO, above 20% of wild-type embryos and *pinhead* or *admp* single mutants showed some mild cases of dorsalization defects (C1 and C2), whereas all of the improved *phΔ49;adΔ11* embryos exhibited more severely dorsalized phenotypes (C3 to C5; Fig. 6E). Furthermore, a reduced amount of injected *bmp2b* MO (0.3 or 0.1 ng) led to marginal dorsalized phenotypes in wild-type and single-mutant embryos, while these subdose injections resulted in hyperdorsalization in improved *phΔ49;adΔ11* mutants (Fig. 6, F and G). These findings indicate that *pinhead* and *admp* cooperatively confer robust resistance to the decrease of BMP signaling during DV patterning.

Because the expression of *pinhead* and *admp* notably decreased in *bmp2b* overexpression embryos (Fig. 4, C to E), these two genes might also play important roles when embryos are challenged with excessive BMP activity. If this deduction is correct, reduced expression of *pinhead* and *admp* should dampen the elevated BMP activity to some extent due to impeded Chd degradation and depletion of these two genes should further stabilize BMP activity profiles during DV patterning. Consistent with these predictions, injection of 10 pg of *bmp2b* mRNA led to severe ventralized phenotypes in above 90% wild-type, *phΔ49*, and *adΔ11* embryos, which were obviously alleviated in about 40% improved *phΔ49;adΔ11* mutants (Fig. 6, H to J). Moreover, our study proved that, similar to Admp, Pinhead also functions in DV patterning via its BMP-like activity (fig. S7E). To explore whether the BMP-like activity of Pinhead and Admp is involved in the robustness of embryonic patterning, we examined the expression patterns of *gsc* and *eve1* in *chd*-depleted embryos at the shield stage. We observed that, upon *chd* depletion, the improved *phΔ49;adΔ11* mutants showed a lower rate of severe ventralized phenotype than wild-type, *phΔ49*, and *adΔ11* embryos (fig. S10, A to C), indicating that the over-activation of BMP signaling induced by *chd* depletion can be appeased through genetic inactivation of both *pinhead* and *admp*. These results also imply that Pinhead and Admp could act as BMP ligands to stabilize embryonic DV patterning. Collectively, these data demonstrate that *pinhead* and *admp* serve as a dual protection system for the robustness of embryonic patterning by buffering against disturbances in the dynamic BMP signaling (Fig. 6K).

DISCUSSION

Robustness is a ubiquitous property in organisms that allows a system to maintain its functions despite external and internal perturbations. These robust biological traits are often selected through evolution and facilitate evolvability (*33*, *34*). One of the best-studied models of robustness in embryonic development is the normal production of gastrula DV patterns after experimental perturbations (*5*–*10*). However, the molecular nature of this self-regulating pattern remains one of the most challenging areas that remain to be delineated in developmental biology. It is well known that a BMP signaling gradient is established through ventral BMP signals and their dorsally expressed antagonist Chd, which forms along the DV axis to pattern tissues (*4*). Admp, a BMP-like protein expressed as part of the feedback regulation of the Chd/BMP system on the dorsal side of gastrulating embryos, is an appealing candidate in ensuring embryonic self-regulation (*8*, *12*). Robustness can be enhanced by an "alternative" or "fail-safe" mechanism, where multiple means achieve a specific function, and the failure of one of them can be overcome by the others (*33*). However, whether there is an alternative mechanism to support the substantial DV polarity remains to be determined.

A previous study revealed that zebrafish *admp* morphants have an almost normal distribution of Chd protein (*17*). Consistent with this observation, the morphology and DV polarity are not affected in the *adΔ11* mutants generated in this present study, suggesting that the loss of Admp function may be quickly compensated for by other BMP-like members. *Xenopus* ONT1, an olfactomedin-class secreted protein, was demonstrated to contribute to the robust stability of axial patterning with Admp in a synergistic manner (*12*).

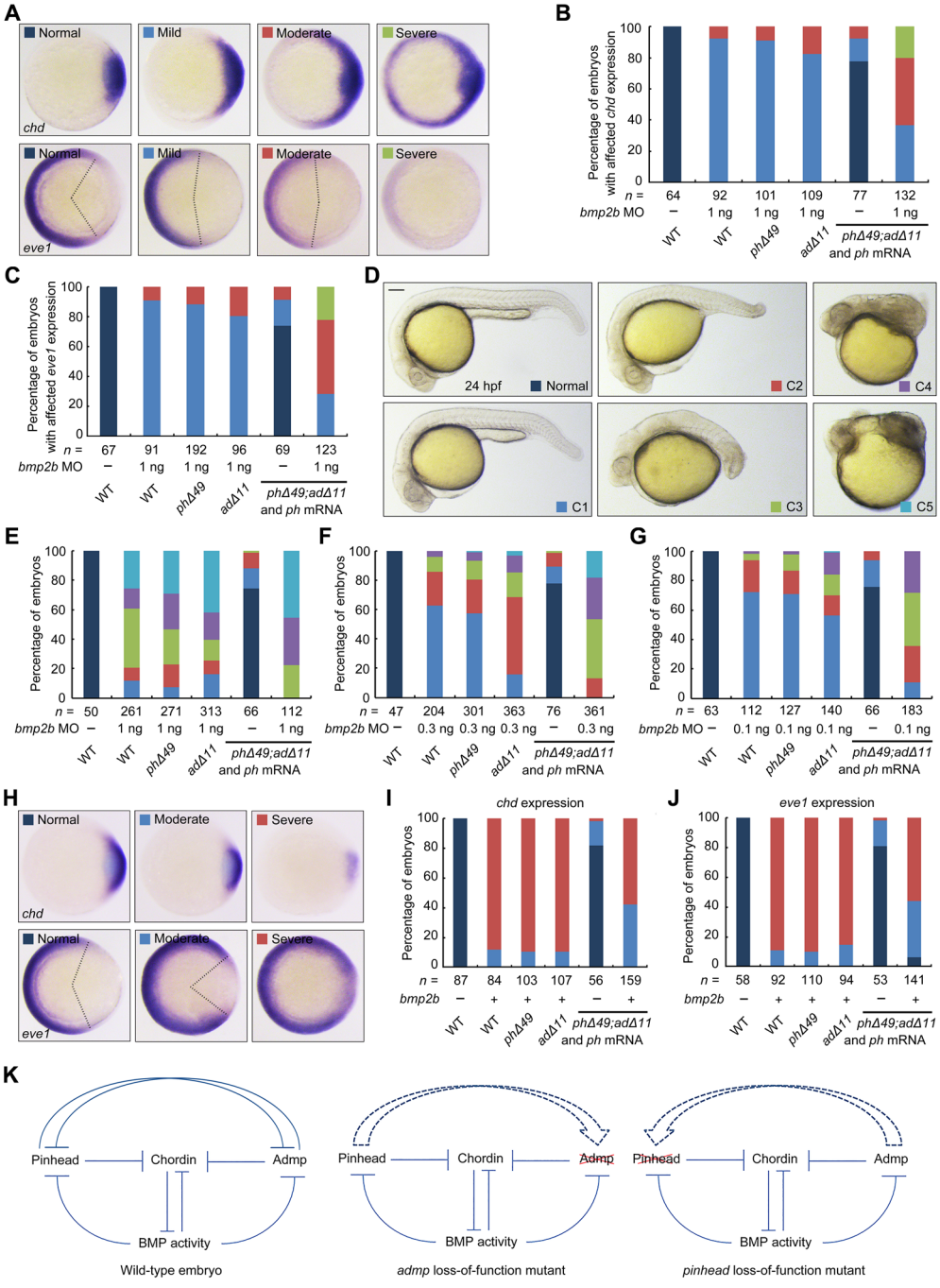

Fig. 6. The *pinhead* and *admp* genes function together to buffer against fluctuations in BMP activity. (**A** to **C**) The expression patterns of dorsal and ventral markers in the indicated embryos injected with *bmp2b* MO. The expression patterns of *chd* and *eve1* were categorized as shown in (A), and the ratios were presented in (B) and (C). Note that injection of 1 ng of *bmp2b* MO into improved *phΔ49;adΔ11* mutant embryos (injected with 100 pg of *pinhead* mRNA) led to much more severe dorsalized phenotypes at the shield stage than wild-type control and single-mutant embryos. (**D** to **G**) Double depletion of *pinhead* and *admp* strongly enhanced *bmp2b* MO-induced dorsalization. Indicated embryos were injected with different doses of *bmp2b* MO (1, 0.3, or 0.1 ng) at the one-cell stage and imaged at 24 hpf. Representative dorsalized morphologies (C1 to C5) are shown in (D), and their ratios are shown in (E) to (G). Scale bar, 100 μm. (**H** to **J**) Double depletion of *pinhead* and *admp* stabilized DV patterns when BMP activity was elevated. Indicated embryos were injected with 10 pg of *bmp2b* mRNA at the one-cell stage and harvested at the shield stage for in situ hybridization with *chd* and *eve1* probes (H). Their ratios of the categorized expression patterns of *chd* and *eve1* are shown in (I) and (J). (**K**) Proposed model of the alternative mechanism for the robustness of embryonic patterning that couples *pinhead* and *admp* with system control based on opposing regulation of BMP signaling and *pinhead/admp* expression. In wild-type embryos, the expression of *pinhead* and *admp* is repressed by each other and by BMP/Smad pathways (the left panel). The negative feedback loop between *pinhead/admp* and BMP signals plays an important role in buffering against fluctuations in dynamic BMP signaling during DV axis formation (left panel). Meanwhile, when the function of *pinhead* or *admp* decreased or failed, the "seesaw"-like expression of these two genes will provide a well-orchestrated alternative mechanism for embryonic self-regulation (the middle and right panels). The arrows with dashed outlines in the middle and right panels indicate the quick up-regulation of *pinhead* or *admp* expression to compensate for the genetic loss of the other gene.

However, unlike Admp protein, ONT1 has no BMP ligand activity and acts as a secreted scaffold that enhances Chd degradation by facilitating enzyme-substrate association. The attenuation of ONT1 causes an increase in Admp expression but still leads to dorsalization phenotypes in *Xenopus* embryos (*12*), suggesting that ONT1 and Admp have non-overlapping functions during DV axis formation. In this study, our data indicate that zebrafish *pinhead* encodes a secreted BMP ligand with ventralizing functions during zebrafish embryo development. *pinhead* mutants had no DV pattern defects because the enhanced expression of *admp* fully compensated for the gene loss. Conversely, *pinhead* also responds to the decrease or depletion of *admp* to stabilize axial formation. Therefore, the "seesaw"-like expression of *pinhead* and *admp* establishes a well-orchestrated alternative mechanism for the robust generation of the DV axis. In addition, similar to Admp, Pinhead acts as a scaffold that promotes metalloproteinase-mediated Chd degradation. Thus, this alternative mechanism is mediated by the remarkable molecular similarities between Pinhead and Admp.

In *Ciona* embryos, *pinhead* is expressed in the posterior ventral epidermal cells, and MO-mediated gene knockdown experiments revealed that *pinhead* functions in the DV axis formation of the trunk epidermis (*23*). In *Xenopus* embryos, *pinhead* is expressed in the anterior neural plate of the neurula and genetic manipulation by MO injection showed that *pinhead* is a key regulator of head development (*22*). Because of a lack of expression of *pinhead* in the epidermal cells and the neural plate during zebrafish embryo development, it is reasonable that we found no defects in the formation of epidermal and neural tissues in our *pinhead* mutants.

An important unanswered question in developmental biology is how a self-differentiating morphogenetic field is established in the developing embryos. Classic embryological studies have demonstrated that *admp* expression is repressed by BMP signaling, and transcriptional up-regulation of *admp* plays a key role in compensating for the depletion of ventrally expressed BMPs (*8*, *28*). Likewise, *pinhead* expression is remarkably increased in embryos injected with *bmp2b* MO or treated with BMP inhibitors, while it notably decreased in embryos overexpressing *bmp2b*. Although a rescuing amount of *pinhead* mRNA had been introduced into *pinhead* and *admp* double mutants, these embryos were more fragile to disturbances in the dynamic BMP signaling gradient, indicating that the opposing transcriptional regulation between *pinhead*/*admp* and ventral BMP signals serves as a negative feedback mechanism and is responsible for the robust pattern formation. On the basis of these observations, we hypothesize a new framework, where the alternative mechanism is coupled with system feedback controls to ensure embryonic self-regulation. This working hypothesis is further reinforced by the identification of functional Smad1/5 binding elements in *pinhead* and *admp* enhancers. However, it has been reported that *admp* expression is decreased in *pinhead* morphants, and *pinhead* expression is suppressed in *admp*-depleted *Ciona* embryos during DV axis formation of the trunk epidermis (*23*). Furthermore, BMP signaling has no effect on *admp* expression but is required for *pinhead* expression in *Ciona* embryos (*23*). Therefore, it is possible that the effects of BMP signaling on *pinhead* and *admp* expression may be context dependent.

Expression of *admp* has been observed in the dorsal organizer (*13*, *14*). ONT1, which has been proposed to stabilize axial formation by restricting Chd activity, is also expressed on the dorsal side (*12*). In addition to the ventral and lateral region, *bmp2b* is also expressed in the dorsal organizer, where organizer-derived BMP2b represses *chd* transcription and helps control the Chd gradient during gastrulation of zebrafish embryos (*17*). It will be interesting to investigate whether organizer-specific *bmp2b* functions in the robust stability of DV patterning. However, our study showed that the expression of *bmp2b* in both the ventrolateral region and the dorsal organizer was not affected by single depletion of *pinhead* or *admp*, suggesting that *bmp2b* may not be involved in the compensatory mechanism for the robustness of embryonic patterning.

Our study revealed that *pinhead* is expressed in the ventrolateral margin of zebrafish gastrulas. The mutually exclusive expression and shared functions of *pinhead* and *admp* suggest that Pinhead can diffuse to the dorsal side as an extracellular signaling molecule, which is indirectly confirmed by the compensatory effects of *pinhead* up-regulation in *admp* mutants. We observed an efficient secretion and a long-range diffusion of Pinhead-GFP fusion proteins in the developing embryos. In embryos, a subset of extracellular secreted factors, such as *xolloid-related*, *twisted gastrulation*, and *crossveinless* 2, function ventrally to promote BMP signaling through a variety of ways. The expression of these genes is positively regulated by BMPs (*4*, *11*), ruling out any potential compensatory roles they may have buffering morphogen profiles against variations. Meanwhile, BAMBI and Sizzled, secreted feedback BMP antagonists, are expressed on the ventral side as part of the BMP synexpression group and shape the BMP signaling gradient (*35*–*38*). These BMP inhibitors may play additional roles ensuring reproducible DV patterns in the face of natural fluctuations (*4*). However, considering normal epidermal DV patterning occurs in BMP4/7-depleted dorsal halves of split *Xenopus* embryos and the formation of extra tails when cells from the ventral margin are transplanted into the animal pole of host zebrafish embryos (*8*, *10*), an additional BMP-like member is likely up-regulated in the ventral region to compensate for deficiencies in BMP activity. Whether expression of *pinhead* is induced in the bisected embryos or the grafts to preserve the ventral identity remains to be determined.

In summary, this present study suggests that *pinhead* and *admp* serve as an alternative mechanism of embryonic self-regulation, where the functions of these two genes can be restored by modular feedbacks when one component fails. It is important to note that this alternative mechanism is coupled with system control on the basis of the opposing regulation of BMP signaling and *pinhead*/*admp* expression for coping with environmental perturbations. Pinhead is the only known BMP member expressed in the ventrolateral region that is suppressed by BMP signaling. However, no expressed sequence homologous to *pinhead* has been found in birds and mammals (*22*, *23*). The identification of other BMP members with functions overlapping with Admp in animals that have lost *pinhead* gene over the course of evolution will be important for increasing our understanding of the molecular mechanism underlying self-regulative DV patterning.

MATERIALS AND METHODS

Zebrafish strains

Embryos and adult fish were raised and maintained under standard laboratory conditions. Wild-type embryos were obtained from natural matings of Tubingen zebrafish. Studies in this manuscript involving zebrafish embryo collection and analyses were in full compliance with the Institutional Animal Care and Use Committee at the Institute of Zoology, Chinese Academy of Sciences (permission number IOZ-13048).

Generation of zebrafish mutant lines using Cas9/gRNA system

Mutant *pinhead* and *admp* lines were generated using the CRISPR-Cas9 system as previously described (*39*). Two guide RNAs (gRNAs) were designed to target the sequences 5′-GGAGGTTGTGTGCTC-GTG-3′ and 5′-GGTCGGAGGCGATCAGG-3′ within the first exon of the *pinhead* and *admp* loci, respectively. The Cas9 mRNA and gRNA were synthesized in vitro and coinjected into one-cell stage wild-type embryos. For screening of the mutant alleles, the genomic regions surrounding gRNA-targeted sequences were amplified by PCR with the following primers: for *pinhead* mutants, 5′-CATGTGGATTAAACACAAAGGC-3′ (forward) and 5′-GAA-ATACTGTAAATGGATTGAACGT-3 (reverse); for *admp* mutants, 5′-TCAGGATCTCCTCGAGGACCACC-3′ (forward) and 5′-TTAT-CTTACATTTGTCGAAGAAG-3′ (reverse). The amplified DNA fragment was purified for enzymatic digestion with T7 endonuclease I (M0302, New England BioLabs) or subjected to Sanger sequencing.

Confirmed founders were crossed to wild-type animals to raise F1 carriers for each mutant. Homozygous mutants were obtained by incrossing F1 fish carrying mutated genomic DNA. *adΔ11* homozygous mutant embryos were injected with Cas9 mRNA and *pinhead* gRNA to generate germline mutants for *pinhead* in an *adΔ11* mutant background. F1 animals were obtained by crossing the founders and *adΔ11* homozygous mutants. Homozygous *phΔ49;adΔ11* double mutants were obtained from the offspring of the $phΔ49^{-/-};adΔ11^{-/-}$ adults.

Constructs

Zebrafish *pinhead* was cloned into pCS2(+) vectors containing a C-terminal HA or FLAG tag for eukaryotic expression. For Pinhead-GFP, the sequence encoding GFP protein was inserted downstream from the *pinhead* coding sequence with an "EFLQDIIDGSPGLE" linker separating the fluorescent protein and the Pinhead protein. C-terminal epitope-tagged Admp, Chd, Noggin1, and Bmp1a were cloned in pCS2-Flag, pCS2-HA, or pCS2-Myc vectors. All the resulting constructs were confirmed by sequence analysis.

Cell lines and transfections

HEK293T cells were cultured in Dulbecco's modified Eagle's medium (DMEM) supplemented with 10% fetal bovine serum in a 37°C humidified incubator with 5% CO_2. Transfection was performed using Lipofectamine 2000 (11668019, Invitrogen) according to the manufacturer's instructions. Once the HEK293T cells transfected with constructs expressing secreted proteins, such as Pinhead, Chd, and BMP1a, reached 80% confluency, they were washed three times with phosphate-buffered saline (PBS) and cultured in serum-free DMEM for 24 hours. CM was then collected from each sample and centrifuged at 3000*g* for 5 min, filtered through a 0.22-μm filter, and concentrated to 10% of the original volume using Centriplus concentrators (Amicon).

RNA and MO microinjection

Capped mRNAs were synthesized in vitro for *pinhead*, *pinhead*-HA, *pinhead*-GFP, *mCherry*-CAAX, *admp*, *bmp2b*, and *gfp* from the corresponding linearized plasmids using the mMessage mMachine kit (Ambion). The following MOs were synthesized by Gene Tools and resuspended in nuclease-free water: *ph* MO (5′-ACTGACAG-CAGTAAATCCATAGTCC-3′), *admp* MO (*ad* MO; 5′-TGGA-CAACATTGTAAAGAACATTGC-3′) (*14*), *bmp2b* MO (5′-CGC-GGACCACGGCGACCATGATC-3′) (*30*), and *chd* MO (5′-ATC CACAGCAGCCCCTCCATCATCC-3′) (*29*). The mRNA and MOs were injected into the yolk, while plasmid DNA was injected into the cytoplasm of one-cell stage embryos.

RNA probe synthesis and WISH

Digoxigenin–uridine triphosphate–labeled and fluorescein-labeled antisense RNA probes were transcribed using the MEGAscript Kit (Ambion) according to the manufacturer's instructions. WISH was performed according to previously published methods (*39*). For double in situ hybridization, anti–digoxigenin-peroxidase (POD) (11633716001, Roche) and anti–fluorescein-POD (11426346910, Roche) were used as primary antibodies to detect digoxigenin-labeled *pinhead* probe and fluorescein-labeled *gsc* probe, respectively.

Embryonic treatment

To block BMP signaling, embryos were treated with 10 μM dorsomorphin (P5499, Sigma) or 5 μM DMH1 (D8946, Sigma) at the 1K-cell stage in the dark, and then were collected at the shield stage for WISH.

Real-time quantitative PCR

Real-time quantitative PCR (qPCR) was performed to check mRNA expression levels of the tested genes. Total RNA was extracted with Trizol (Invitrogen) and complementary DNAs were synthesized with high-efficiency reverse transcriptase Revertra Ace (Toyobo). A Biorad CFX96 PCR system was employed to perform real-time PCR using SYBR Premix Ex Taq dye (Takara). The primer sequences were as follows: for β-*actin*, 5′-ATGGATGATGAAATTGCCG-CAC-3′ (forward) and 5′-ACCATCACCAGAGTCCATCACG-3′ (reverse); for *gsc*, 5′-GAGACGACACCGAACCATTT-3′ (forward) and 5′-CCTCTGACGACGACCTTTTC-3′ (reverse); for *chd*, 5′-TAGACTGCTGTAAGGAGTGTCCTC-3′ (forward) and 5′-CCATGAAGTCCTCTATGCATTCCG-3′ (reverse); for *eve1*, 5′-GCGAACTGGCGGCAGCCCTTAACT-3′ (forward) and 5′-GTAGGTCGATGGAGGCAGGTGCAAAG-3′ (reverse); for *vent*, 5′-GCAAGTTCTCAGTGGAGTGGCT-3′ (forward) and 5′-TCTGATCGCAGGTGAATTTGGT-3′ (reverse); for *pinhead*, 5′-AGTCCAGTGAATGTAGATG-3′ (forward) and 5′-CTCTCGCAG-ACCTTCATACAG-3′ (reverse); for *admp*, 5′-TCATGTTGTATG-CAATGTTC-3′ (forward) and 5′-GTGACTCCGTCGACATCAGC-3′ (reverse); for *gfp*, 5′-TGAAGTTCATCTGCACCACCGGCAA-3′ (forward) and 5′-CCAGGATGTTGCCGTCCTCCTTGAA-3′ (reverse).

Immunoprecipitation and Western blot analysis

For immunoprecipitation assays, HEK293T cells were transfected with the indicated plasmids. Cells were harvested 48 hours after transfection and lysed with TNE lysis buffer [10 mM tris-HCl (pH 7.5), 150 mM NaCl, 2 mM EDTA, and 0.5% Nonidet P-40] containing a protease inhibitor cocktail. Immunoprecipitation assays were performed on lysates and collected CM as previously described (*39*).

For immunoblotting, affinity-purified anti-Flag (F2555, Sigma), anti-HA (CW0092A, CW), anti-Myc (M047-3, MBL), anti–phospho-Smad1/5/8 (9511, Cell Signaling Technology), anti-Smad1/5/8 (ab72504, abcam), anti–phospho-Smad2/3 (3101, Cell Signaling Technology), anti-Smad2/3 (3102, Cell Signaling Technology), anti-Chd (GTX128209, GeneTex), and anti–β-actin (SC1615, Santa Cruz Biotechnology) antibodies were used.

Immunofluorescence analysis

Embryos were collected at the shield stage, fixed in 4% paraformaldehyde overnight, washed with PBS containing 0.1% Tween 20 for 30 min, blocked with 1% bovine serum albumin for 1 hour at room temperature, and then incubated with anti–phospho-Smad1/5/8 (1:200; 9511, Cell Signaling Technology) for 24 hours at 4°C. After washing with PBS three times for 5 min each, the samples were incubated with a donkey anti-rabbit secondary antibody conjugated to DyLight 594 (1:500; 711-585-152, Jackson ImmunoResearch) overnight at 4°C. All immunofluorescence images were captured using a Nikon A1R+ confocal microscope with the same settings for all samples within each experiment.

Prokaryotic expression and protein purification

An in-frame insertion of the cDNA of the full human Smad1 gene with a glutathione *S*-transferase (GST) tag into the plasmid pGEX-4 T-1 was performed, and the resulting recombinant plasmid was transformed into *Escherichia coli* strain BL21. GST-tagged Smad1 protein expression was induced using 1 mM isopropyl-β-D-thiogalactopyranoside, and the resulting protein was purified with glutathione Sepharose 4B beads (GE Healthcare) according to the manufacturer's instructions. Protein was digested by thrombin and dialyzed against buffer I [10 mM tris-HCl (pH 7.5), 1 mM dithiothreitol (DTT), and 0.2 M NaCl] at 4°C overnight. Proteins were brought to a final concentration of 200 μg/ml.

Electrophoretic mobility shift assays

Electrophoretic mobility shift assays were performed as follows. Mixtures of purified Smad1 (10 ng) protein and 0.5 ng of carboxyfluorescein (FAM)–labeled probes were incubated at room temperature for 30 min in a 10-μl reaction volume. The reaction buffer contained 25% glycerol, 50 mM KCl, 0.5 mM EDTA, 10 mM DTT, and 5 mM tris-HCl and had a pH of 8.0. The mixtures were resolved on a 6% nondenaturing polyacrylamide gel (60:1 acrylamide-to-bisacrylamide ratio) containing 5% glycerol in 0.5× tris-borate EDTA buffer. The gels were visualized using a Typhoon FLA9500 Scanner.

Dual luciferase reporter assays

For detection and quantification of *pinhead* or *admp* promoter activity in zebrafish embryos, the luciferase reporter construct DNA was mixed with Renilla luciferase reporter DNA in a ratio of 10:1. Wild-type and mutant embryos were injected with 100 pg of the DNA mixture at the one-cell stage. To inhibit BMP signal transduction, embryos were treated with or without 5 μM DMH1 at the 1K-cell stage and then lysed with passive lysis buffer at the shield stage for detecting luciferase activities. Each luciferase reporter assay was performed in triplicate, and the data represent the mean ± SD of three independent biological repeats after normalization to *Renilla* activity.

Statistical analysis

Student's *t* tests (two-tailed, unequal variance) were performed to analyze all datasets (Microsoft Excel software). At a minimum, experiments were performed in triplicate. All the group values are expressed as the mean ± SD. Results were considered statistically significant at $P < 0.05$.

SUPPLEMENTARY MATERIALS

Supplementary material for this article is available at http://advances.sciencemag.org/cgi/content/full/5/12/eaau6455/DC1

Fig. S1. Pinhead is a secreted BMP-like ligand.
Fig. S2. Axial formation is normal in *pinhead* homozygous mutants.
Fig. S3. DV polarity is not affected in *admp* homozygous mutants.
Fig. S4. The activities of Admp and Chd are not obviously affected by the addition of C-terminal epitopes.
Fig. S5. Simultaneous deletion of *pinhead* and *admp* causes defects in dorsal- and ventral-related tissues.
Fig. S6. Double inactivation of *pinhead* and *admp* induces severe dorsalization in embryos.
Fig. S7. *pinhead* and *admp* have similar function to rescue the DV defects in *phΔ49;adΔ11* mutants.
Fig. S8. Overexpression of BMP2b in wild-type, *phΔ49* mutant, or *adΔ11* mutant embryos leads to similar ventralized phenotypes.
Fig. S9. Potential Smad1/5-bound GC-rich elements in *admp* and *pinhead* enhancers.
Fig. S10. *pinhead* and *admp* stabilize embryonic patterning in *chd* morphants.
Data file S1. The uncropped blots for the Westerns and immunoprecipitations.

View/request a protocol for this paper from *Bio-protocol*.

REFERENCES AND NOTES

1. M.-J. Goumans, A. Zwijsen, P. Ten Dijke, S. Bailly, Bone morphogenetic proteins in vascular homeostasis and disease. *Cold Spring Harb. Perspect. Biol.* **10**, a031989 (2018).
2. Z. Li, Y.-G. Chen, Functions of BMP signaling in embryonic stem cell fate determination. *Exp. Cell Res.* **319**, 113–119 (2013).
3. S. C. Little, M. C. Mullins, Bone morphogenetic protein heterodimers assemble heteromeric type I receptor complexes to pattern the dorsoventral axis. *Nat. Cell Biol.* **11**, 637–643 (2009).
4. Y. G. Langdon, M. C. Mullins, Maternal and zygotic control of zebrafish dorsoventral axial patterning. *Annu. Rev. Genet.* **45**, 357–377 (2011).
5. N. Barkai, B. Z. Shilo, Robust generation and decoding of morphogen gradients. *Cold Spring Harb. Perspect. Biol.* **1**, a001990 (2009).
6. H. Spemann, H. Mangold, Induction of embryonic primordia by implantation of organizers from a different species. 1923. *Int. J. Dev. Biol.* **45**, 13–38 (2001).
7. S. Koshida, M. Shinya, T. Mizuno, A. Kuroiwa, H. Takeda, Initial anteroposterior pattern of the zebrafish central nervous system is determined by differential competence of the epiblast. *Development* **125**, 1957–1966 (1998).
8. B. Reversade, E. M. De Robertis, Regulation of ADMP and BMP2/4/7 at opposite embryonic poles generates a self-regulating morphogenetic field. *Cell* **123**, 1147–1160 (2005).
9. K. Joubin, C. D. Stern, Molecular interactions continuously define the organizer during the cell movements of gastrulation. *Cell* **98**, 559–571 (1999).
10. A. Agathon, C. Thisse, B. Thisse, The molecular nature of the zebrafish tail organizer. *Nature* **424**, 448–452 (2003).
11. M.-C. Ramel, G. R. Buckles, K. D. Baker, A. C. Lekven, WNT8 and BMP2B co-regulate non-axial mesoderm patterning during zebrafish gastrulation. *Dev. Biol.* **287**, 237–248 (2005).
12. H. Inomata, T. Haraguchi, Y. Sasai, Robust stability of the embryonic axial pattern requires a secreted scaffold for chordin degradation. *Cell* **134**, 854–865 (2008).
13. M. Moos Jr., S. Wang, M. Krinks, Anti-dorsalizing morphogenetic protein is a novel TGF-beta homolog expressed in the Spemann organizer. *Development* **121**, 4293–4301 (1995).
14. Z. Lele, M. Nowak, M. Hammerschmidt, Zebrafish *admp* is required to restrict the size of the organizer and to promote posterior and ventral development. *Dev. Dyn.* **222**, 681–687 (2001).
15. B.-Z. Shilo, M. Haskel-Ittah, D. Ben-Zvi, E. D. Schejter, N. Barkai, Creating gradients by morphogen shuttling. *Trends Genet.* **29**, 339–347 (2013).
16. R. Dosch, C. Niehrs, Requirement for anti-dorsalizing morphogenetic protein in organizer patterning. *Mech. Dev.* **90**, 195–203 (2000).
17. Y. Xue, X. Zheng, L. Huang, P. Xu, Y. Ma, Z. Min, Q. Tao, Y. Tao, A. Meng, Organizer-derived Bmp2 is required for the formation of a correct Bmp activity gradient during embryonic development. *Nat. Commun.* **5**, 3766 (2014).
18. X.-H. Feng, R. Derynck, Specificity and versatility in TGF-β signaling through Smads. *Annu. Rev. Cell Dev. Biol.* **21**, 659–693 (2005).
19. E. M. De Robertis, Evo-devo: Variations on ancestral themes. *Cell* **132**, 185–195 (2008).
20. E. Bier, E. M. De Robertis, BMP gradients: A paradigm for morphogen-mediated developmental patterning. *Science* **348**, aaa5838 (2015).
21. K. Miyazono, Y. Kamiya, M. Morikawa, Bone morphogenetic protein receptors and signal transduction. *J. Biochem.* **147**, 35–51 (2010).
22. S. Kenwrick, E. Amaya, N. Papalopulu, Pilot morpholino screen in *Xenopus tropicalis* identifies a novel gene involved in head development. *Dev. Dyn.* **229**, 289–299 (2004).
23. K. S. Imai, Y. Daido, T. G. Kusakabe, Y. Satou, Cis-acting transcriptional repression establishes a sharp boundary in chordate embryos. *Science* **337**, 964–967 (2012).

24. Y. Kishimoto, K. H. Lee, L. Zon, M. Hammerschmidt, S. Schulte-Merker, The molecular nature of zebrafish swirl: BMP2 function is essential during early dorsoventral patterning. *Development* **124**, 4457–4466 (1997).
25. A. Rossi, Z. Kontarakis, C. Gerri, H. Nolte, S. Hölper, M. Krüger, D. Y. R. Stainier, Genetic compensation induced by deleterious mutations but not gene knockdowns. *Nature* **524**, 230–233 (2015).
26. R. Jasuja, N. Voss, G. Ge, G. G. Hoffman, J. Lyman-Gingerich, F. Pelegri, D. S. Greenspan, *bmp1* and *mini fin* are functionally redundant in regulating formation of the zebrafish dorsoventral axis. *Mech. Dev.* **123**, 548–558 (2006).
27. F. Rentzsch, J. L. Zhang, C. Kramer, W. Sebald, M. Hammerschmidt, Crossveinless 2 is an essential positive feedback regulator of Bmp signaling during zebrafish gastrulation. *Development* **133**, 801–811 (2006).
28. V. Willot, J. Mathieu, Y. Lu, B. Schmid, S. Sidi, Y.-L. Yan, J. H. Postlethwait, M. Mullins, F. Rosa, N. Peyriéras, Cooperative action of ADMP- and BMP-mediated pathways in regulating cell fates in the zebrafish gastrula. *Dev. Biol.* **241**, 59–78 (2002).
29. A. Nasevicius, S. C. Ekker, Effective targeted gene 'knockdown' in zebrafish. *Nat. Genet.* **26**, 216–220 (2000).
30. Y. Imai, W. S. Talbot, Morpholino phenocopies of the *bmp2b/swirl* and *bmp7/snailhouse* mutations. *Genesis* **30**, 160–163 (2001).
31. D. W. Laux, J. A. Febbo, B. L. Roman, Dynamic analysis of BMP-responsive smad activity in live zebrafish embryos. *Dev. Dyn.* **240**, 682–694 (2011).
32. T. Fei, K. Xia, Z. Li, B. Zhou, S. Zhu, H. Chen, J. Zhang, Z. Chen, H. Xiao, J.-D. J. Han, Y.-G. Chen, Genome-wide mapping of SMAD target genes reveals the role of BMP signaling in embryonic stem cell fate determination. *Genome Res.* **20**, 36–44 (2010).
33. H. Kitano, Biological robustness. *Nat. Rev. Genet.* **5**, 826–837 (2004).
34. H. Kitano, Towards a theory of biological robustness. *Mol. Syst. Biol.* **3**, 137 (2007).
35. C. Niehrs, N. Pollet, Synexpression groups in eukaryotes. *Nature* **402**, 483–487 (1999).
36. U. Martyn, S. Schulte-Merker, The ventralized ogon mutant phenotype is caused by a mutation in the zebrafish homologue of Sizzled, a secreted Frizzled-related protein. *Dev. Biol.* **260**, 58–67 (2003).
37. S. C. Little, M. C. Mullins, Extracellular modulation of BMP activity in patterning the dorsoventral axis. *Birth Defects Res. C Embryo Today* **78**, 224–242 (2006).
38. H. X. Lee, A. L. Ambrosio, B. Reversade, E. M. De Robertis, Embryonic dorsal-ventral signaling: Secreted frizzled-related proteins as inhibitors of tolloid proteinases. *Cell* **124**, 147–159 (2006).
39. S. Wei, M. Dai, Z. Liu, Y. Ma, H. Shang, Y. Cao, Q. Wang, The guanine nucleotide exchange factor Net1 facilitates the specification of dorsal cell fates in zebrafish embryos by promoting maternal β-catenin activation. *Cell Res.* **27**, 202–225 (2017).

Acknowledgments: We are grateful to members of the Q. Wang laboratory for assistance and discussion. **Funding:** This work was supported by grants from the National Key Research and Development Program of China (2016YFA0100503 and 2018YFA0800200), the National Natural Science Foundation of China (81921006, 31571501, and 91739101), and the Strategic Priority Research Program of the Chinese Academy of Sciences (XDA16000000). **Author contributions:** Y.Y. performed most of the experiments and analysis. Y.Y. and Q.W. conceived and designed the experiments and wrote the manuscript. Q.W. supervised the entire project. All authors reviewed and commented on the manuscript. **Competing interests:** The authors declare that they have no competing interests. **Data and materials availability:** All data needed to evaluate the conclusions in the paper are present in the paper and/or the Supplementary Materials. Additional data related to this paper may be requested from the authors.

Submitted 2 July 2018
Resubmitted 30 April 2019
Accepted 29 October 2019
Published 18 December 2019
10.1126/sciadv.aau6455

Citation: Y. Yan, G. Ning, L. Li, J. Liu, S. Yang, Y. Cao, Q. Wang, The BMP ligand Pinhead together with Admp supports the robustness of embryonic patterning. *Sci. Adv.* **5**, eaau6455 (2019).

Science Advances

The BMP ligand Pinhead together with Admp supports the robustness of embryonic patterning

Yifang Yan, Guozhu Ning, Linwei Li, Jie Liu, Shuyan Yang, Yu Cao and Qiang Wang

Sci Adv **5** (12), eaau6455.
DOI: 10.1126/sciadv.aau6455